Abstract

Due to the increasing environmental awareness of society and administration, a great number of regulations became effective over the last years in order to preserve natural resources restricting and limiting industrial waste, especially when spills affect aqueous systems. This fact has contributed to the development of a large amount of research programs to come across new methods and processes to monitor and reduce contaminants present in wastewater.

Among the variety of contaminants present in industrial effluents, heavy metals are the most hazardous as this compounds are biomagnified and can reach human organism. One of the methods developed for reducing heavy metal concentration in wastewater is biosorption.

Biosorption process monitoring has led to the development of sensor arrays or electronic tongues. These kinds of sensors require exhaustive training through the analysis of huge sets of standards, which is time, effort and reagent consumptive.

This project is addressed on the optimization of a Sequential Injection Analysis (SIA) prototype built to prepare automatically random generated known training standards and monitor bioprocess absorption to model sensor's response.

In this phase of optimization a miniature spectrometer is assembled to the SIA tubing to monitor flow response in real time of a colorant solution. Spectroscopic analysis also allows monitoring traces of reagent remaining on the system.

Calibration and cleaning routines will be designed to ensure reproducibility. Moreover, automatic preparation of standards will be discussed.

Table of contents

1. Glossary

Avg: Average

C: Closed

DQA: Data Acquisition System

FIA: Flow Injection Analysis

LOD: Limit of Detection

LOQ: Limit of Quantization

NO: *Normally open*

NC: *Normally closed*

O: Open

PR: Phenol Red

S/N: Signal to noise ratio

SIA: Sequential Injection Analysis

UV: Ultraviolet

UV-Vis: Ultraviolet Visible

2. Preface

2.1. Project background

The present Degree Final Project is a contribution to the research project: “Desarrollo de Tecnología a Escala Piloto para Depuración de Aguas Contaminadas con Iones Metálicos mediante Residuos Agroalimentarios (TECMET)” funded by Ministerio de de Economía y Competitividad, Madrid, 2013-2015. Project CTM2012-37215-C02-02 and to the research project “SINTESIS VERDE DE NANOPARTICULAS METALICAS A PARTIR DE AGUAS ACIDAS DE MINA Y EXTRACTOS DE RESIDUOS AGROALIMENTARIOS” funded by Ministerio de Economía y Competitividad, Madrid and FEDER funds, EU, 2016-2018. Project CTM2015-68859-C2-2-R (MINECO/FEDER).

2.2. Incentive

This project’s incentive is setting the operation conditions and obtaining reproducible routines to elaborate automatically standards automatically by using a stirrer cell implemented in the SIA prototype.

Therefore, flow UV-Visible spectroscopy will be utilised to monitor colorant reagent streams, in order to optimize the SIA parameters.

3. Introduction

This project follows the project “Diseño y construcción del prototipo de un sistema de Análisis de Inyección Secuencial para la monitorización de procesos mediante lenguas electrónicas” by (de Lamo 2014) and the contributions made in “Optimització d’un sistema de monitorització de processos basat en anàlisi per injecció seqüencial (SIA) by (Escudé 2015), and it is made simultaneously to “Estudio de la fluidica asociada a la optimización de un sistema de análisis por inyección secuencial (SIA)” by (Núñez 2016). These projects contribute on the optimization process of the SIA prototype.

3.1. Objectives

The main objective of this project is determining flow parameters by UV-Visible spectroscopy for proper automatic sample and/or sample generation in the stirrer cell.

A secondary objective is obtaining reliable and reproducible procedures for calibration, priming and cleaning routines.

3.2. Project Scope

This project comprises script programming, colorant reagent characterization through spectroscopy, dispersion studies, minimum volume calculations, signal analysis and automatic dilution procedures.

4. Flow Analysis

4.1. What is flow analysis?

As exposed in (Christian 2003), a large amount of analytical chemistry processes and goals are completely included in flow techniques, which are used to improve the capabilities of several other measurement procedures.

Flow methods are recognized as excellent tools for solution management and are used to perform all types of operations, allowing fast and precise measurements using small samples and minimizing the reagent consumption, one of the goals of green chemistry. Furthermore, flow analysis methods can be miniaturized and automated in order to reduce operator error, while enabling multiple analyses being performed.

Examples of flow analysis techniques are FIA and SIA.

4.2. Analytical procedure automation

Science and technology development over the last decades have generated new tendencies and needs for analytical chemistry. On the one hand, more sophisticated equipment improves conventional methods with less aggressive procedures and an enhancement on performance.

On the other hand, environmental quality data grows in size as new procedures are being developed. One of the reasons of designing and implementing a SIA system was to develop an automatic training method for monitoring biosorption in wastewater analysis with electric tongues.

(Nuñez *et al.* 2013) in their application of electric tongues for monitoring nitrogen compounds in waters establish that in order to train the sensor array forming the electronic tongue an artificial neuronal network (AAN) had to be configured.

The AAN response model was constructed from an appropriate set of calibration solutions, also named as training subset, and then tested with a separate subset of additional 15 samples, known as the external test subset, and finally tested with random composition samples.

The elaboration of all the required samples manually would suppose a large time and resource wasting. As will be explained in sections 4.3 and 4.4, sequential injection analysis (SIA) systems can economise the procedure through less reagent consumption.

One of the parameters that will be tested in section 9 will be the ability and reproducibility of elaborating samples automatically on the prototype's stirring cell by UV-Visible spectroscopy. Once working conditions are determined, sensor arrays can be connected to the system and be trained automatically on the same manifold.

4.3. Flow Injection Analysis (FIA)

Flow injection analysis is one of the most studied and developed continuous flow techniques. It was documented by J.Ruzicka and E.H. Hansen in 1975.

Originally, flow injection analysis was conceived as an essay monitoring tool, significantly decreasing operation times. However, research and development of the different methods allowed enhancing the performance of spectroscopy or electrochemical systems among others.

As (Kikas 2014) remarks, FIA technique consists in the injection of prefixed small volumes in the order of microlitres inside a continuous stream of another solution named carrier solution. The controlled dispersion of the injected sample zone and the reproducible timing of its movement are the main characteristics. This stream will be constantly driven into a detector system which will detect any of the flow or other non-flow related properties. This can be shown in Figure 4-1.

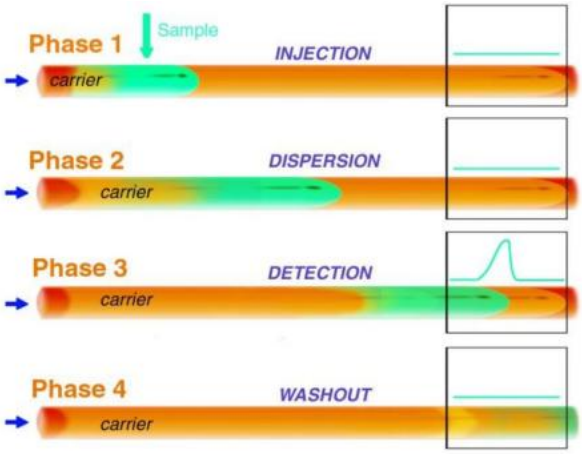

Figure 4-1 Four phases of Flow Injection (Kikas 2014)

Carrier solution stream will generate what is called a baseline, which is the detector response when no analyte is present in the system. When an analyte is injected, the difference between the current response and the baseline generates a response peak proportional to the particular property of the analyte and it is different for every compound.

Dispersion results from two processes, as (Larsen and Harvey 2013) specify: convection,

due to the flow carrier stream and, diffusion, due to the concentration gradient between the sample and the carrier stream. Convection occurs by laminar flow, as wall friction slows down the outer layers of the fluid while the central ones move as twice as the stream's linear velocity. Diffusion helps to maintain the sample's flow profile.

Diffusion occurs both parallel (axially) and perpendicular (radially) to the direction in which the stream is moving, as can be seen in Figure 4-2

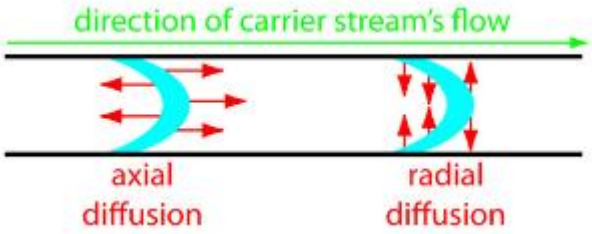

Figure 4-2 Stream diffusion

A basic FIA system consists in a pumping device capable of impelling the flow stream and maintaining constant hydrodynamic properties, an injection system connected to the circuit in such a way flow characteristics remain unaltered, and finally a detection system. An schematic of this configuration is shown in Figure 4-3

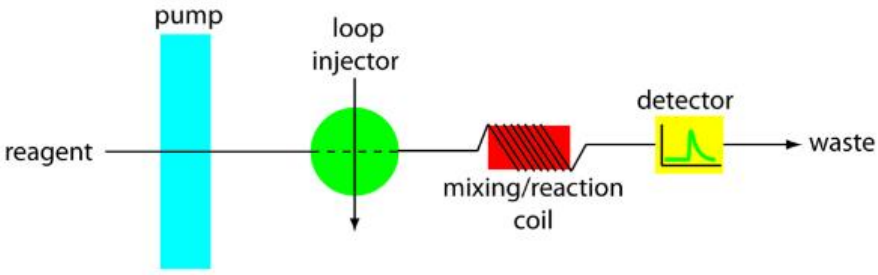

Figure 4-3 Basic FIA manifold (Larsen and Harvey 2013)

Every different application for a FIA system requires its own way for the analyte to arrive to the detector in a form that can give a valid response. Per example, in conductimetry the sample must remain undiluted through its transportation. For spectrophotometry the analyte must be converted into a measurable compound.

4.4. Sequential injection analysis (SIA)

Sequential injection analysis was born in 1989 as an alternative to FIA for process monitoring. Technological advances emphasized two major impediments as (Pasekova *et al.* 1999) remark: the requirement for a different manifold for each analytical method and the

relatively high maintenance of peristaltic pumps.

Similarly to FIA, SIA depends on the principle of controlled partial dispersion, in combination with forward and reversed flow through a multiposition valve, which facilitates the use of different reagents and methods without changes in the manifold.

The core of SIA systems is a multiposition valve operating in synchronisation with a pump. Connecting to various sample and reagent reservoirs allows aliquots being drawn into a holding coil, while the pump is operating in reverse. Then on forward propulsion the stream is dispersed into a zone of detectable product. A schematic view is shown in Figure 4-4

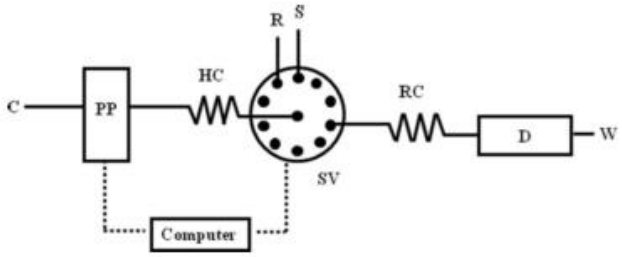

Figure 4-4 Configuration of a basic SIA system. C: carrier, PP: pumping device; SV: selection valve; HC: holding coil; RC: reaction coil; D: detector; W: waste; R: reagent; S: sample (Pinto *et al.* 2011)

One condition for detection in SIA systems is that the flow through the cell should be propelled with low pressure pumps. UV-visible, infrared luminescence and atomic spectroscopy, and even electrochemical measurements are included among the utilised detection methods.

In FIA systems the sample is completely surrounded by reagent, while in SIA the sample and reagent zones are stacked consecutively and as the flow moves through the instrument, the zones disperse inside each other. This can be accomplished either by the use of a reaction coil or a mixing cell.

(Pasekova *et al.* 1999) also reported some authors like Gübeli using syringe pumps for propulsion in SIA, or like Cladera, utilizing an autoburette for the same function, as both instrumentations are capable of moving flows bidirectionally.

On the other hand, SIA requires some elements that a FIA system can operate without, as mentioned in (Baxter and Christian 1996): a computer with sophisticated software and a precise pump. High precision pumping is necessary because all volumes are defined by pump timing rather than by a physical loop. Autoburettes though, accomplish this role as volumes are defined by piston, and a stepper motor.

5. Ultraviolet-Visible Spectroscopy

5.1. An overview on spectroscopy

Spectroscopic methods are based on the interaction of ultraviolet, visible and infrared radiation with matter. This interaction is described by the properties of both particles and waves. Light is a form of energy consisting of oscillating electric and magnetic fields that propagate through space with constant velocity, and is also a beam of energetic particles called photons.

5.1.1. Electromagnetic radiation

As discussed previously, light waves can be represented as oscillating perpendicular electric and magnetic fields. The oscillations are sinusoidal in shape as shown in Figure 5-1.

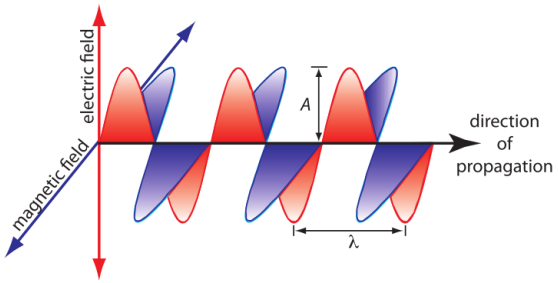

Figure 5-1 Electromagnetic Wave form (Harvey 2009)

Now some definitions can be made accurately. The wavelength λ can be defined as the peak-to-peak distance between two successive maxima. The standard unit of wavelengths is the meter (m), but in terms of spectroscopy is frequent the use of nanometre (nm). The amplitude of the wave is defined as the maximum of the vector from the origin to a point displacement of the oscillation (Robinson *et al.* 2005). The frequency *v* is the number of oscillations in the electric field per unit time. The common unit of frequency is the hertz (s^{-1}). The wavelength of light is related to its frequency by Equation 5-1

$$c = \lambda * \nu \qquad \text{Equation 5-1}$$

where c is the speed of light in vacuum, 2.997 x 10^8 m/s. In vacuum, the speed of light is a maximum and does not depend on the wavelength. As frequency is determined by the source and does not vary, when light passes through other materials its speed is decreased, thus the wavelength must decrease.

The frequency and wavelength of electromagnetic radiation vary over many orders of

magnitude. It is common to divide the electromagnetic spectrum into different regions as shown in Figure 5-2

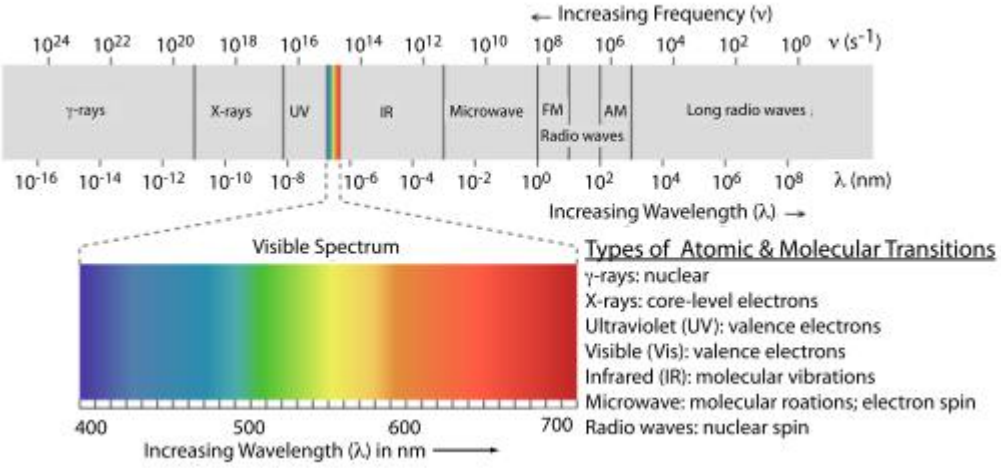

Figure 5-2 Electromagnetic spectrum (Harvey 2009)

The important regions for UV-visible spectroscopy are ultraviolet and visible spectrums.

5.1.2. Radiation Interaction with matter

According to (Harvey 2009), the phenomena of absorption is produced because of the attenuation of a radiation's intensity at selected wavelengths when a beam goes through a sample. Thus, some of the photons are absorbed by a sample and their energy is transferred to electrons, promoting them to a higher energy excited state. For molecules, the energy required for electronic excitation lies in the visible and UV ranges. Molecules possess several possible rotational and vibrational states, so the absorption is produced over a wide range of wavelengths, which is called an absorption band.

Spectroscopic measurement is possible only if the photons interaction leads to a change in one or more of the characteristic properties of electromagnetic radiation: energy, velocity, amplitude, frequency among others.

5.2. Beer – Lambert – Bouguer Law

5.2.1. Basic definitions

(Robinson *et al.* 2005) define the radiant power *P* of a beam of light as the energy of the beam per second per unit area. A related quantity is the intensity *I* which is the power per unit solid angle. Both power and intensity are related to the square of the amplitude of the light wave, and the absorption laws can be written in terms of either power or intensity.

When light passes through an absorbing sample, the intensity of the light emerging from the sample is decreased. Calling I_0 the intensity of the beam before entering the sample, and I the intensity after passing through, the transmittance T is defined as the ratio of I to I_0.

Transmittance is the fraction of the original light that passes through the sample. To study the quantitative absorption of radiation is useful to define another quantity, the absorbance A where

$$A = log\left(\frac{I}{I_0}\right) = log\left(\frac{1}{T}\right) = -\log T$$ Equation 5-2

When no light is absorbed, $I = I_0$ and $A = 0$.

5.2.2. Beer's Law

Following a similar approach of (Harvey 2009), when electromagnetic radiation passes through an infinitesimally thin layer of sample of thickness *dx*, it experiences a decrease in its intensity of *dI*, as shown in Figure 5-1

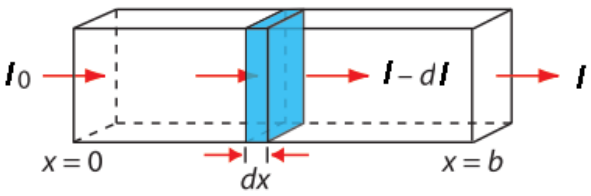

Figure 5-3 Beer - Lambert law factors modified from (Harvey 2009)

The fractional decrease in intensity is proportional to the sample's thickness and the analyte concentration *C*. According to (Robinson *et al.* 2005), the proportional relationship between sample thickness (the pathlength) and absorbance at constant concentration was discovered by P. Bouguer in 1729 and J. Lambert in 1760.

Therefore, the intensity drop can be expressed as

$$-\frac{dI}{I} = \alpha C dx$$ Equation 5-3

Where α is a proportionality constant. Integrating the left side of Equation 5-1 over the entire sample

$$-\int_{I_0}^{I}\frac{dI}{I} = \alpha C\int_{0}^{b} dx$$

$$\ln \frac{I_0}{I} = \alpha b C$$

Converting from ln to log, and substituting in Equation 5-2 results in

$$A = \varepsilon b C \qquad \text{Equation 5-4}$$

Where *b* is the pathlength, usually in cm, and ε is the molar absorptivity coefficient, which has units of cm^{-1} M^{-1}. The molar absorptivity is proportional to the probability that the analyte absorbs a photon of a given energy. As a result, ε depends on the wavelength of the absorbed photon.

Equation 5-4 establishes the linear relationship between absorbance and concentration, and is more commonly known as the Beer-Lambert law, or Beer's law.

5.2.3. Limitations to Beer's Law

Beer's law works best when the concentration is less than about 0.01 M. At high concentrations of analyte, its individual particles no longer behave independently of each other and start interacting between themselves. In this case interactions may change analyte's absorptivity.

Another important factor is that absorptivity depends on the samples's refractive index, which varies with the analyte's concentration. Therefore in flow systems, it is significant choosing the right carrier solution and reagent medium to avoid adding further error.

Some instrumentation limitations also induce deviation from Beer's law as (Harvey 2009) suggested. The first limitation is that Beer's law assumes that the radiation reaching the sample is of a single wavelength. However, wavelength selectors pass radiation with a small effective bandwidth.

The second contribution is due to imperfections in the wavelength selector that allows light to enter the instrument and reach the detector without passing through the sample. This phenomenon is called Stray Radiation. Inside this definition it can also be included the radiation not being isolated properly from the detector. Stray radiation minimisation will be discussed later on.

5.3. Spectroscopic detectors

In this section a small overview on spectroscopic detectors will be explained. Specific information about the equipment utilised on this project will be given in the next section.

Equipment miniaturisation has led to a new era of modular spectrometers.(Harvey 2009) classifies these spectrometers as Diode Array Spectrometers.

Conventional instruments have a single detector, so only a wavelength at a time can be monitored. The use of many photodiodes instead of a single photomultiplier results in an array of detectors that can record an entire spectrum in less than a second.

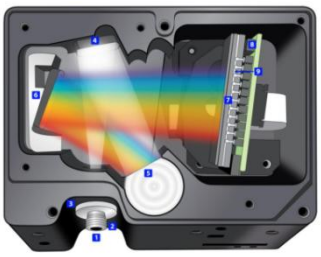

Figure 5-4 Flame-S detector overview (Ave 2015)

Figure 5-4 is an overview of the detector utilised in this project. As shown in (Ave 2015), light arriving from the sample reflects from a mirror as a collimated beam toward the grating, where it is dispersed. Radiation is then again reflected form a focusing mirror, which directs radiation one wavelength apart to the detector array.

One of the advantages (Harvey 2009) reports for diode array spectrometers is the speed of data acquisition, which allows to collect several spectra for a single sample. Individual spectra are added and averaged to obtain the final spectrum. This signal averaging improves a spectrum's signal-to-noise ratio, smoothing the data. Figure 5-5 shows the effects of signal averaging.

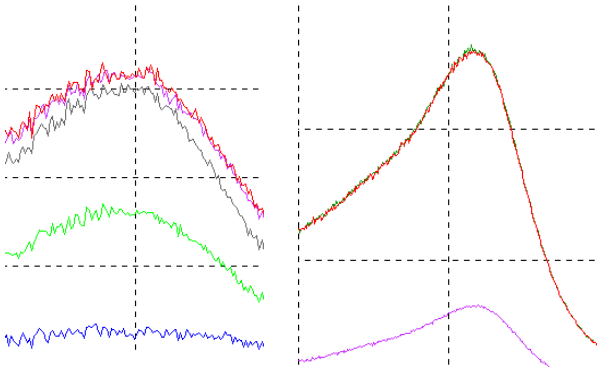

Figure 5-5 Left: Non averaged spectra. Right: 15 scans averaged

The signal-to-noise ratio (S/N) after n scans is described by **¡Error! No se encuentra el origen de la referencia.**, where S_x/N_x is the signal-to-noise ratio for a single scan.

$$\frac{S}{N} = \sqrt{n}\frac{S_x}{N_x}$$ Equation 5-5

However, the principal disadvantage (Harvey 2009) has found for these spectrometers is that the effective bandwidth per diode, on a photodiode array, is nearly an order of magnitude larger than that for a high quality monochromator.

5.4. Sample Cells

Samples are usually in the liquid or solution state, and are placed in cells constructed with UV-Visible transparent materials. A sample cell must achieve two major requirements.

It's trivial to assume that cell's material must let all the radiation to reach the sample and pass through it. Despite this condition, not all materials behave the same way. For radiation in the visible range (400-700 nm wavelength), materials such as quartz, glass and plastic are appropriate. When working at shorter than 300 nm wavelengths quartz or fused-silica cells must be used. Other materials show a significant absorption in this range and interfere in measurements.

The other requirement the cell must accomplish is chemical compatibility. Material of the cell must be chosen to resist the chemical attack of the utilised solvents and samples. (FIAlab 2015) provides a table of compatibility for SMA-Z-Cells.

When Beer's law was defined in 5.2.2, Equation 5-4***¡Error! No se encuentra el origen de la referencia.*** introduced the variable pathlength *b*. Pathlength is directly proportional to the analyte's absorbance, hence increasing the pathlength will yield to higher absorbance, which is useful when analyzing diluted solutions or gas samples.

6. Sequential injection analysis (SIA) prototype

The prototype consists in three parts: the autoburette, the main manifold and a computer. A schematic view of the whole system is represented in Figure 6-1.

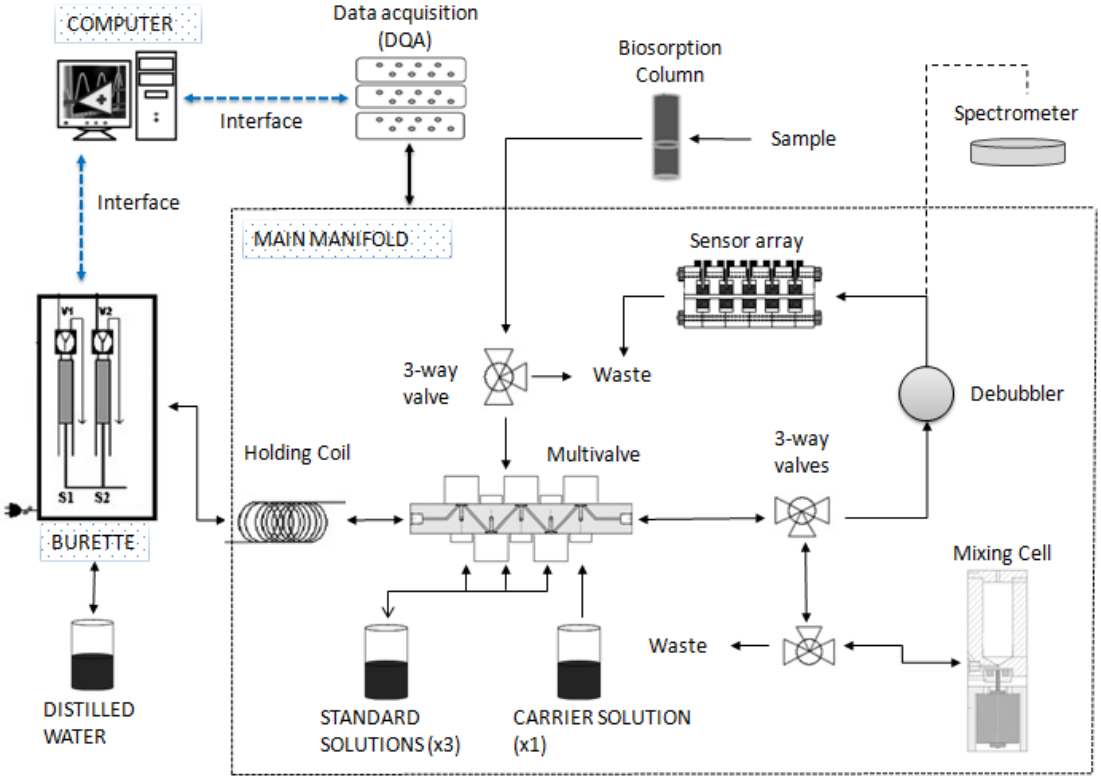

Figure 6-1 SIA schematic modified from (Núñez 2016)

A computer is required to command both the autoburette and the elements on the main assembly through the utilization of the program called LabVIEW (National Instruments). Data acquisition (DQA) from the sensor array can also be controlled with this software. However, DQA and sensors will not be discussed in this project.

Although the spectrometer is external to the prototype, it has been added to the schematic. It is also controlled by the computer but uses its own software detailed in 7.2.

Figure 6-2 displays the complete assembly in the laboratory.

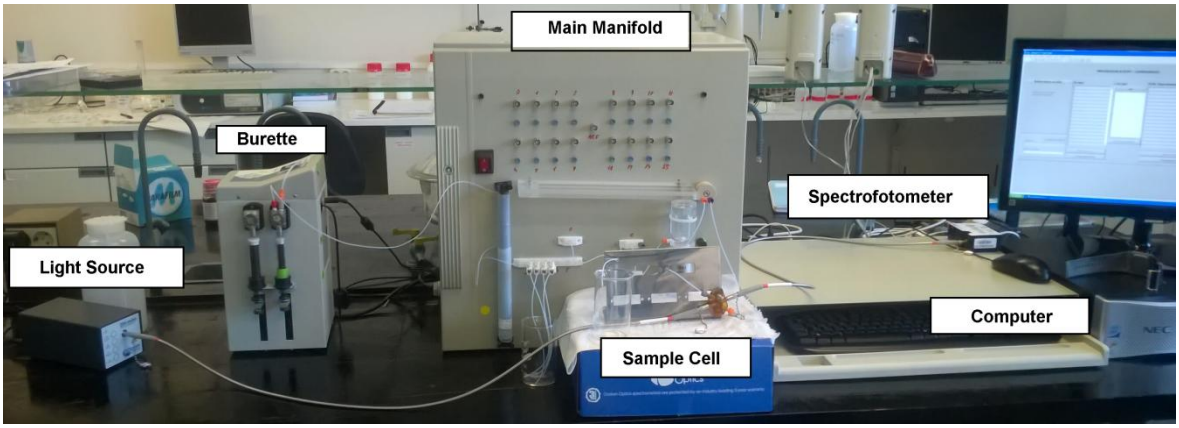

Figure 6-2 SIA assembly

6.1. MultiBurette 2S

Crison Multiburette 2S is the pumping device of the prototype. It can operate two syringes simultaneously, though only one has been used in this project (total volume of 5 ml). Operation conditions of the system will be explained later on in section 8.

The utilisation of a multiburette accomplishes one of the most relevant SIA systems requirements. SIA systems must be able to guarantee bidirectional flow movement. The burette has a 40000 steps motor that moves a piston up or down. That means the minimum volume it can move is 1/40000 of the syringe total volume.

When turning on the burette the motor activates lowering the piston to the bottom of the syringe, filling it, which is why it is recommended to always ensure there's water to avoid introducing air into the system.

Figure 6-3 MultiBurette 2S

In figure Figure 6-3 the current display of the burette is shown. On the right side, the 5 ml syringe utilised for the parameterization of the system. (Núñez 2016) found that lesser volume syringes were more accurate. Each syringe has two input/output valves. The right one is connected to a distilled water tank and the left one, to the holding coil. Commonly, the right entry is named Out and the left entry is named In.

6.2. Main Manifold

6.2.1. Holding Coil

Its function is to avoid that any reagent arrives to multiburette's syringes that could contaminate the SIA system. When a reagent must be inserted into the system the burette has to lower the plunger, aspirating liquid from the coil and allowing the entry of reagents from the multivalve ports.

The holding coil is made from 1 mm internal diameter PTFE tube coiled to a solid plastic rod in order to keep a security and contention volume to store reagents and protect the pumping device.

(de Lamo 2014) determines coil's volume from the following expressions:

$$V_{Ring} = \pi(D_{rod} + D_{Tube}) * \frac{\pi {D_{Tube}}^2}{4}$$ *Equation 6-1*

$$V_{Coil} = N_{Rings} * V_{Ring}$$ *Equation 6-2*

$$L_{rod} = N_{Rings} * D_{Tube}$$ *Equation 6-3*

The current holding coil has a total volume of 6 ml and a tube length of 7.64 m. Another holding coil with 12 ml and 15 m is also prepared in the case of using the 10 ml syringe.

6.2.2. Multivalve

The next component following the holding coil is the multivalve. The multivalve replaces the usual rotator valve in SIA systems, reducing times switching valve channels because rotator valves only have one rotation direction.

Multivalve has five flow valves connected to a single central channel. Entrances 1-4 are destined to the insertion of carrier solution, reagents and calibration standards. Number 5 is connected to a 3-way valve where the biosorption column will be connected to, so samples can be monitored punctually

can be monitored punctually.

6.2.3. 3-way valves

The assembly contains three 3-way valves that allow the flow to take different paths through the other components. Figure 6-4 displays the location and numeration of the valves, the holding coil and the mixing cell.

A first valve, labelled 0, is placed over the multivalve and its central port is connected to the port 5. The biosorption column is connected to another port and a waste line on the remaining. This valve allows introducing samples into the system to be analized.

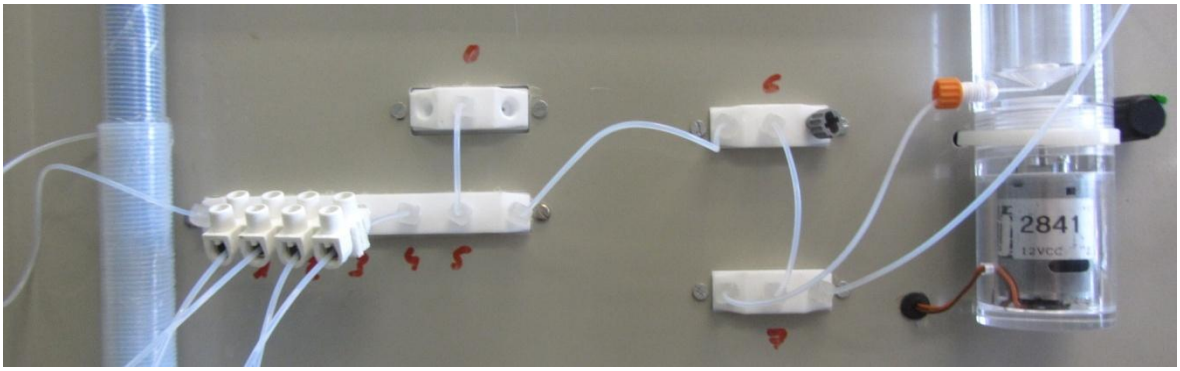

Figure 6-4 SIA front view

The second valve, 6, is connected to the exit of the multivalve and to the third valve. The remaining port is currently unused though it was planned as a waste line.

Finally, the third valve, 7, connects to the mixing cell and to the debubbler. Activating the valve via software the stream goes towards one of these components, blocking its way to the other. As shown in Figure 6-5, valves 0, 6 and 7 have an open entrance, a normally closed entrance and a normally open one.

Figure 6-5 Valve positions (front view)

The central port is always open. Upon activating the valves, the entrances switch to the ON status, opening the normally closed port and closing the normally open. This way flow paths are determined through the SIA system. NC and NO ports are placed as in Figure 6-5 for

valves 6 and 7. For valve 0, the entrances are inverted, so the left one is the NO and the right one is the NC.

6.2.4. Mixing Cell

A stirrer cell was designed to replace the reaction coil. The cell is made of PMMA and has a volume of 15 ml. Mixing is produced activating the motor with a neodymium imant located on the bottom compartment, that induces movement to the stirring bar on the cell. Motor power can be modified moving the knob next to the cell.

Figure 6-6 Mixing Cell

Reagents and carrier solution must be pumped from the holding cell to the stirrer cell. After the pumping, the agitation is activated by the computer until the mixture is completed, and then must be aspirated back to the holding coil in order to be sent to the sample flow cell afterwards.

6.2.5. Debubbler

A membrane debubbler is placed between valve 7 and the detection system in order to eliminate the maximum amount of bubbles contained in the flow stream and avoid interferences on signal measuring.

6.3. Interface: LabVIEW

A user-friendly interface has been designed in LabVIEW to ease the understanding of the commands programmed as well as providing a visual display informing the status of the execution. The created interface also allows controlling and reading graphically the data obtained via the sensor array. However, this function will not be discussed in this project.

6.3.1. Scripts and experiments

Scripts are files that contain the instructions that LabVIEW must execute to activate the prototype's different components. This software's interface makes a distinction between "scripts" and "experiments", though both kinds of files contain orders as defined.

Scripts contain directly the orders the program executes while experiments contain the file path to a set of scripts. This system sets an advantage: programming basic tasks in scripts allows splicing full sets of program into simple routines such as cleaning the mixing cell or priming the multivalve. These routines can be combined in an experiment file, which allowing better understanding of the system and easier task modification. An example will be discussed in 6.3.2.

6.3.2. Programming scripts

Code lines composing program orders can be generalised with the following structure (Table 6-1). Each order starts with a module and then the commands are included in the command list.

Module,	Command list:

Table 6-1 Program order structure (Núñez 2016)

Each module relates to a set of orders relative to a component, and is indicated by a number and all are presented in Table 6-2. Command orders admit adding commentaries separating the text from the command list via tabulations.

Module	Component
1	Valves
2	Burette
3	Time
4	Acquisition
5	Stirrer

Table 6-2 Module description

Next, the set of instructions for each module is described. As data acquisition is not covered

in this document, this module will not be explained.

- **1, Valves**

  Valve commands are used to activate or deactivate the valves, opening or closing paths. The total amount of controllable valve ports is 7, and they are numbered 7 to 0 in Figure 6-4.

7	**6**	**5**	**4**	**3**	**2**	**1**	**0**
0	0	1	0	0	0	0	0

Table 6-3 Valve programming

  Activating 5, for example, requires programming 1,10000: That is, the amount of zeroes that must be added behind is equal to the number of positions between target valve and 0. Following the same procedure, any combination of valves can be opened adding the correspondent 1.
  Instruction 1,0: will close all valves.

- **2, Burette**

  Burette instructions are far more complicated and will be detailed in (Núñez 2016).
  In this project, the only syringe utilised in the burette is the 5 ml syringe, and it is located on the right of the burette (Figure 6-3).

2,	A	E	V.	C.

Table 6-4 Burette general instruction (Núñez 2016)

  Table 6-4 shows the general structure for burette instructions. Using *(Núñez 2016)* notation:
  A indicates the state of the non-used syringe, and its value depends on parameter E.
  E indicates the valve of the syringe that is being used.
  V determines the speed the piston moves.
  C includes a letter: “P” for aspiration and “D” for dispensing followed by the number of steps the motor must move.

- **3, Time**

  Module 3 orders are used to set delay times. The system will wait the amount of seconds indicated in the order until moving forward to the next.
  Time orders follow the general structure presented in Table 6-1 as: 3,X: where X is the amount of time in seconds.

- **5, Stirrer**

On a very similar way to time orders, stirrer orders are 5,0: and 5,1: the last activating the motor and the first deactivating it. Mixing time must be introduced as a time order between the activation and deactivation of the motor.

6.3.3. Executing scripts and experiments

Executing LabVIEW will require pressing  to execute continuously the SIA program.

On the experiment screen of LabVIEW, clicking on the folder icon will prompt a file browser window as in Figure 6-7. Experiments must be loaded from the E folder and scripts from the S folder icons. Otherwise the execution will not work properly.

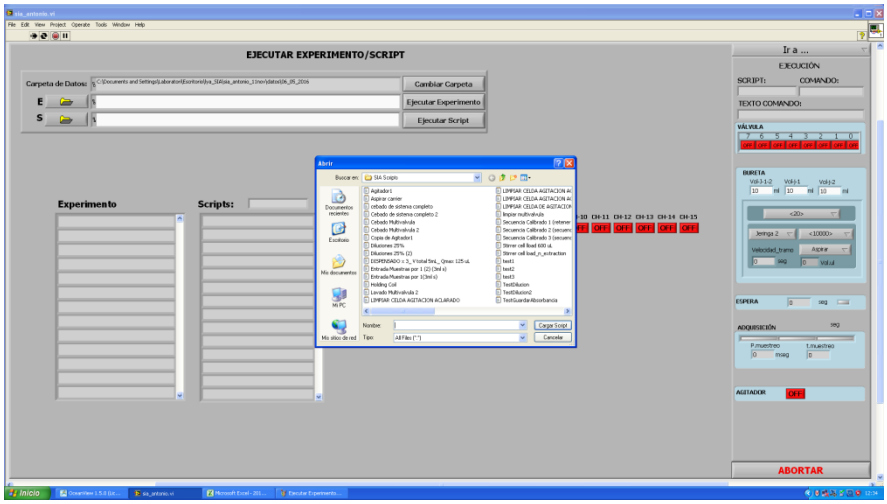

Figure 6-7 Script File Browser

Once the file is selected, pressing the respective execute window will start the execution and will display the command lines below, and monitor the current order with the right side of the screen interface as in Figure 6-8. When valves, the stirrer, or a waiting order are activated, the display will light a green button showing the active component. Otherwise, deactivated components will remain red.

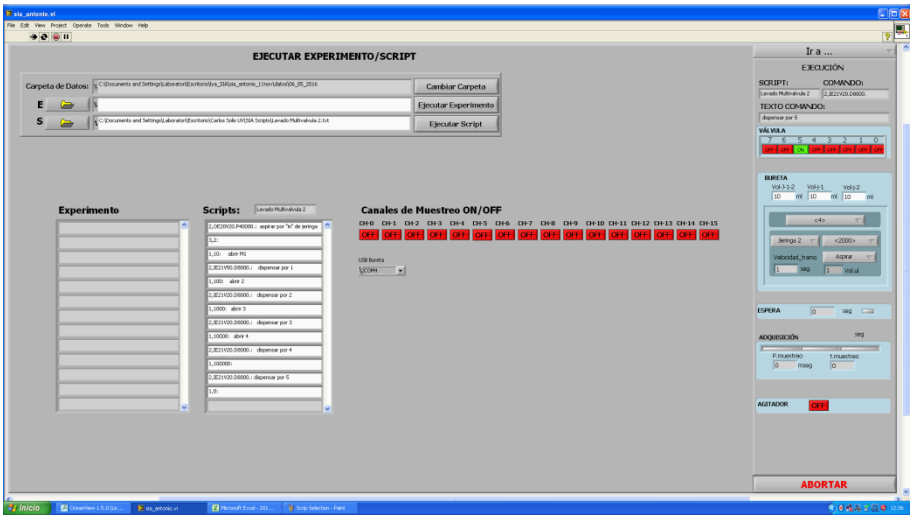

Figure 6-8 Script execution

However, once the execution has started LabVIEW does not allow using any of the other script related interfaces.

7. Flame S Spectrometer

In this section the spectroscopy equipment is described. Figure 7-1 presents the spectroscopy system. All components were provided by Ocean Optics.

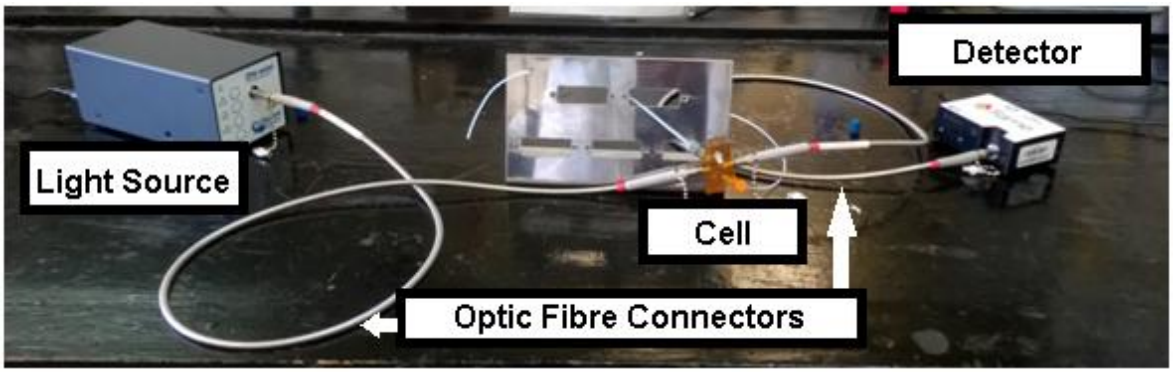

Figure 7-1 Spectroscopy system

The chosen system allows monitoring in real time flow samples, unlike the more traditional spectrometers that require stationary samples in cells to be analyzed; this spectrometer is connected to the SIA's main flow path. The full system display can be seen in Figure 6-2.

7.1. Components

7.1.1. Detector

The flame spectrometer offers a good all-around performance. The detector, a Sony ILX511B linear silicon CCD array, was explained in 5.3.

Figure 7-2 Flame S Spectrometer

Data acquisition is stored connecting the spectrometer to a computer via micro USB-USB connector and executing Ocean View software. Flame S spectrometer has different connection possibilities in order to plug and simultaneously work with other Ocean Optics devices. The optic fibre is attached via the SMA port shown in Figure 7-2.

7.1.2. Sample cell

FIAlab® SMA-Z-10-UL is the sample cell utilised for this project. It is made of PEI resins and has a path length of 10 mm. The optical path is defined by the tube length between the two SMA ports where optic fibre connects (the two middle iron connectors shown in Figure 7-3). Optic fibre is protected from the reagents as SMA ports contain a silica window between two Teflon seals.

Figure 7-3 SMA-Z-10-UL

The cell must be located in angle to ensure an always ascending flow stream in order to let the bubbles exit the optic path. Therefore, flow enters the cell from the orange ferrule and leaves the cell from the grey ferrule.

7.1.3. Light source

DH-mini UV-VIS-NIR Lightsource (Figure 7-4) is an independent radiation source from the spectrometer. The source contains two light bulbs: a Deuterium lamp for UV measurements and a halogen bulb for visible. Additionally has a shutter that can be opened or closed. Closing the shutter while the light sources are working allows storing a dark spectrum.

DH-mini can be controlled both automatically and manually. Automatic function can be controlled with a logical function generator. This option is not used in this project. All options are triggered manually

Figure 7-4 DH-mini UV-VIS-NIR Lightsource

7.1.4. Optic fibre connectors

Two optic fibre QP450-1-XSR connectors are utilized to transmit light from the source to the cell and from the cell to the detector.

7.2. OceanView software

OceanView is a Java-based spectroscopy software by Ocean Optics, and is capable of controlling any Ocean Optics USB spectrometer. The procedure to obtain spectroscopy absorbance measurements will be detailed in this section.

7.2.1. Starting OceanView

Before executing the program, make sure the spectrometer is connected to the computer. If not, the software will simulate a device based on the selected working option. Upon launching the program, the spectroscopy application wizard screen will trigger showing a grid of nine working modes, as can be seen in Figure 7-5.

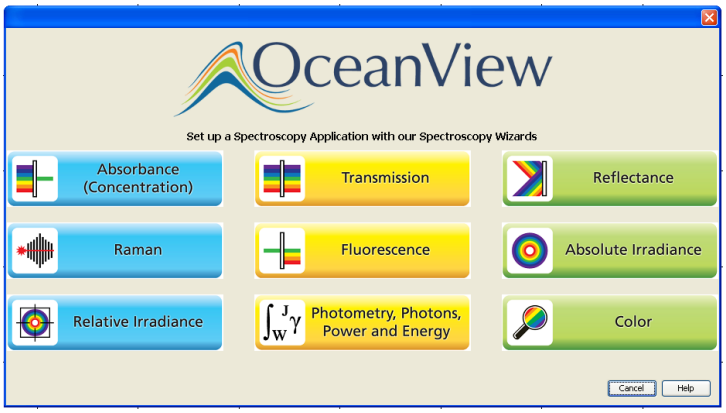

Figure 7-5 Spectroscopy application wizard

Selecting Absorbance (concentration) UV-Vis absorption measurements can be executed. The other options are not explored for this application. When Absorbance (concentration) is selected, Concentration Choice screen pops out offering three options as shown in

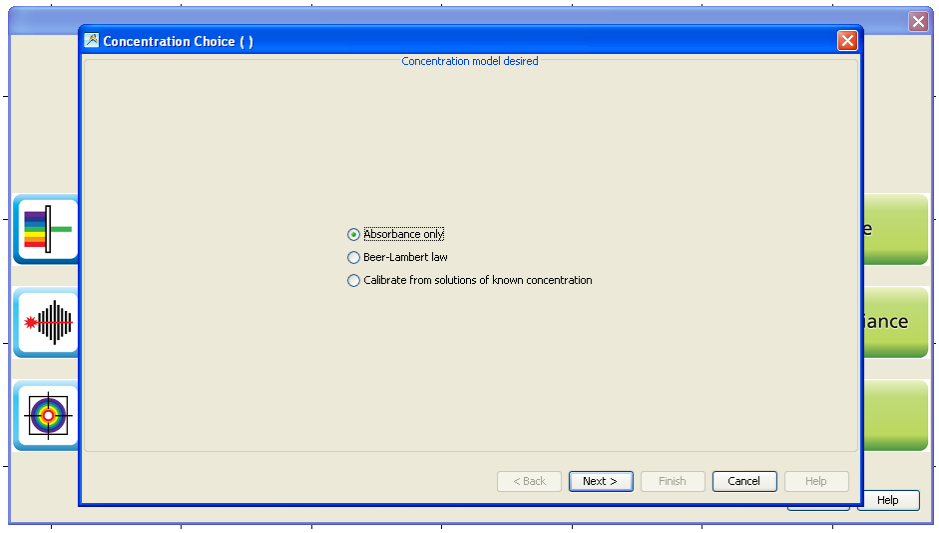

Figure 7-6 Concentration Choice

"Absorbance only" mode only displays and stores absorbance data. "Beer-Lambert law" mode allows calculating concentration at a fixed wavelength once all coefficients in Beer's law are known. "Calibrate from solutions of known concentration" allows storing absorbance-concentration data pairs and create a calibration curve. Absorbance only mode is selected as it allows a better monitoring of spectral data for calibration than calibration mode. However, the last was used briefly during the preliminary tests.

7.2.2. Acquisition parameters

Choosing the working method will led to the Set Acquisition Parameters screen, shown in Figure 7-7. In this screen the user defines the parameters utilised for obtaining spectral data. On the right side of this screen, the user can observe the current spectroscopic lecture.

"Integration time" defines the amount of time utilised to calculate a single spectra, its default value is 100 ms. Clicking in automatic, Ocean View will calculate integration time setting it to the 85% of the spectrometer's dynamic range.

"Scans to average" sets the amount of scans taken for averaging in order to increase the S/N, defined in section 5.3. Integration time and the number of scans total processing time is set to sum less than 1.5 seconds, as acquisition starts to delay considerably over this amount of time.

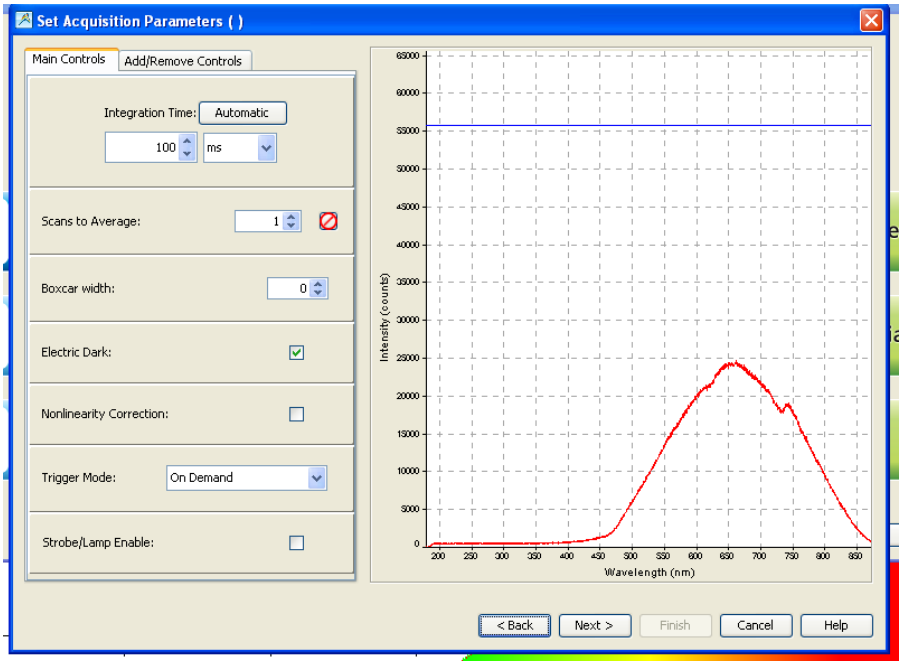

Figure 7-7 Set Aquisition Parameters

7.2.3. Reference and dark spectrum

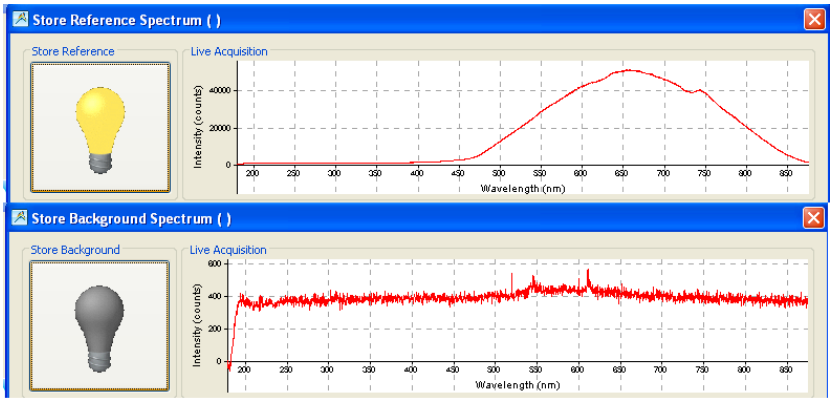

Figure 7-8 Store Reference and Background spectrum

Once acquisition parameters are determined, reference and dark spectrums must be stored in order to be subtracted from the sample's spectrum in order to obtain only analyte's response. Screens from Figure 7-8 appear in order to store spectrums. Reference spectrum is selected pressing the yellow light bulb when the proper lamp has been selected. Dark spectrum is captured closing the shutter on the light source while the lamp is on.

When the spectrums are stored, a new window appears on screen showing the resultant calculated spectrum. This spectrum is obtained through Equation 7-1.

$$A_\lambda = -\log_{10}\left(\frac{S_\lambda - D_\lambda}{R_\lambda - D_\lambda}\right)$$ *Equation 7-1*

Where A_λ is the simple intensity at wavelength λ, D_λ is the dark or background intensity at wavelength λ and R_λ, the reference intensity at wavelength λ.

7.2.4. Wavelength selection

When working in absorbance only mode, to obtain all measurements during a period of time at a fixed wavelength is interesting to work in strip chart mode. This allows isolating the signal for the desired wavelength and plots a graphic with all acquisition data points.

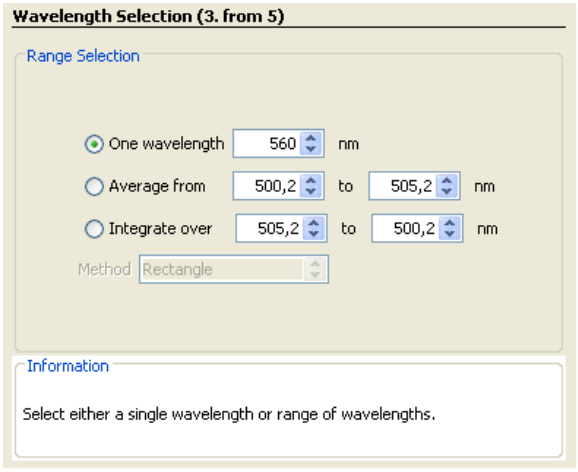

Figure 7-9 Wavelength selection

Figure 7-9 shows the selection wavelength screen where the desired wavelength is selected. Wavelength selection will be discussed in 9.1.

7.2.5. Storing data

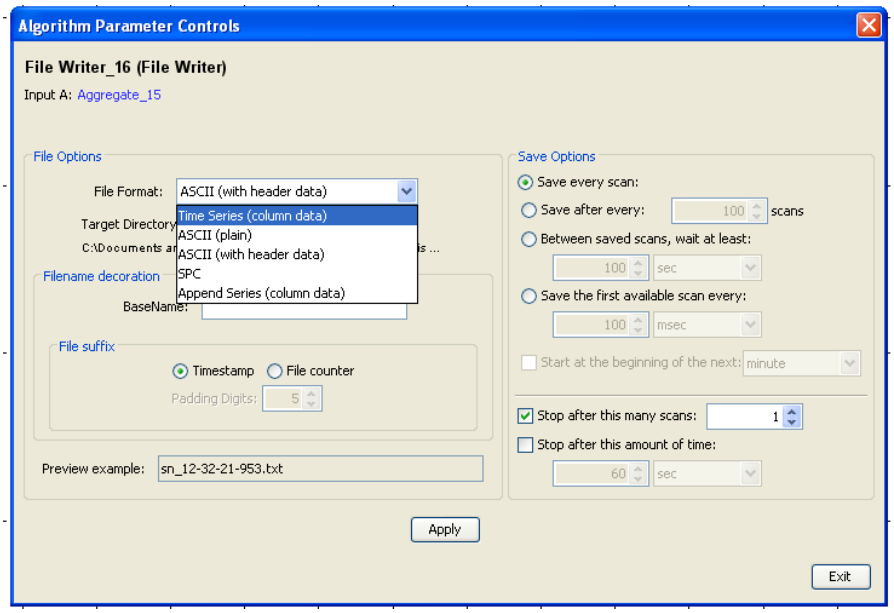

Figure 7-10 Data saving configuration screen

Data saving wizard, displayed in Figure 7-10, permits configuring the file format for the saved data, the target directory where files will be allocated, the file name and an automatic suffix generator for multiple files for the same experiment. In order to save all spectral data inside the same file, Time Series (column data) format will be selected. Saved data will appear tabulated in three columns: acquisition time, active pixels and absorbance value.

Each row will contain a single acquisition time and the measured absorbance at that time. Other file formats generate multiple files for each measurement, which is useless for long running experiments as a large amount of files has to be processed.

This screen also allows configuring the frequency data is written on a file, and programming the duration of file writing.

8. Experimental Procedure

In this section, the experimental procedure utilised will be detailed. In order to be capable of monitoring flow moving through the SIA prototype's tubing, a coloured reagent solution will be analysed by UV-Visible spectroscopy.

8.1. Reagents

A colorant solution of Phenol red will be employed as the optic reagent. Its use for dispersion analysis in flow systems has been described in (del Mar 2004).

Phenol red is a weak organic acid and a reversible pH-sensitive dye. As can be seen in Figure 8-1, Phenol red colour changes when its predominant state is in acidic form or in conjugate base form.

Figure 8-1 Phenol red in: Left: basic medium Right: acid medium

For this project, phenol red will be used in its basic form where its maximum absorption is inside the 550 nm and 560 nm range. (del Mar 2004) sets measurements at 550 nm while (Sochacka 2015) works at 559 nm. (Sochacka 2015) sets the wavelength after analyzing phenol red full absorbance spectrum for both basic and acidic forms in different medium as shown in Figure 8-2. As a part of the experimental procedure, phenol red solutions will be characterized to select the appropriate wavelength.

To preserve phenol red in basic form, al solutions will contain sodium hydroxide 0.1 M as solvent, and sodium hydroxide 10^{-5} M will be the carrier solution.

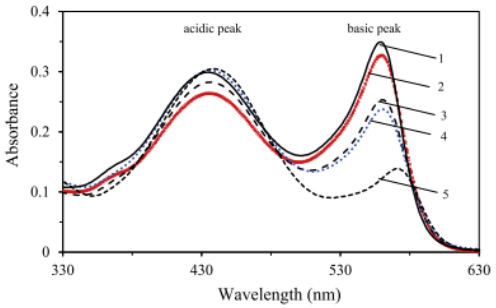

Figure 8-2 Phenol red absorption spectrum (Sochacka 2015)

8.2. Calibration Method

(Robinson *et al.* 2005) define calibration as the process of establishing the relationship between the measured signal and known concentrations of analyte. After establishing this relationship, the concentration of the analyte in an unknown sample can be calculated measuring its response.

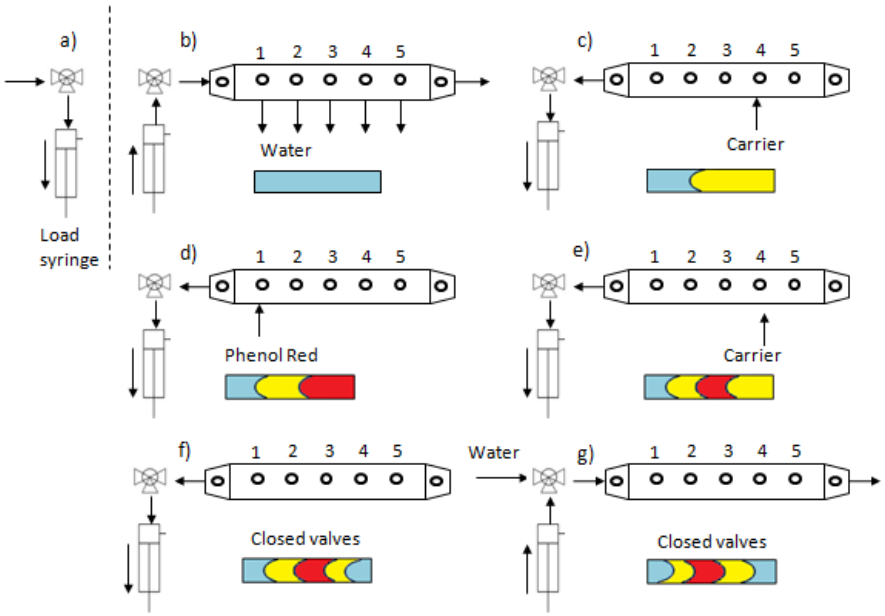

Figure 8-3 Reagent aspiration procedure modified from (Núñez 2016)

Figure 8-3 displays a general procedure to introduce samples on the system. First, the burette is loaded with distilled water from the distilled water tank and is dispensed through the multivalve, cleaning the tubing from previously utilised solutions. Next, a volume of carrier is aspirated through multivalve port 4. Then, samples are aspirated via one of the entries 1-3 of the multivalve, as shown in Figure 8-4 , more carrier solution is injected afterwards.

Figure 8-4 Standard entries

The aspirated volume is stored in the holding coil. Reagents are introduced between two volumes of carrier to prevent high degrees of dispersion. Finally, it is dispensed to the detection system or the stirring cell, depending on the kind of determination.

8.2.1. External Calibration

Standards are injected into the system utilizing ports 1-3 of the multivalve, while the carrier solution is aspirated from port 4. Each standard is introduced separately, that is, the next solution is not introduced into the system until the last has been sent to the detector.

8.2.2. Internal Calibration

A concentrated standard will be injected and then diluted to the same concentration as the standards utilised in 8.2.1. Following a similar procedure to Figure 8-3 carrier is aspirated from 4 and samples from 1-3. Reagents are dispensed into the mixing cell and then the rest of the needed volume for the dilution is added from carrier solution, to preserve basic medium.

8.3. Standards preparation

Calculations for each solution can be found in Annex A.

8.3.1. Phenol red stock solution

Following the procedure described by (del Mar 2004) and (Vindevoghel 2005), a stock solution of phenol red 400 ppm in NaOH 0.1 M was prepared.

0.100 g of phenol red is weighed and added to a volumetric flask of 250 ml. Then 1.00 g of sodium hydroxide pellets is weighed and dissolved in Milli-Q water, and then added to the volumetric flask. Make up to the mark with Milli-Q water.

8.3.2. Sodium hydroxide solution 0.1 M

4 g of sodium hydroxide are weighed on a beaker and then dissolved in Milli-Q water. Then it is added to a volumetric flask of 1000 ml. Then it is made up to the mark with Milli-Q water.

8.3.3. Sodium hydroxide carrier solution

25 µl from the 0.1 M NaOH solution are put on a 250 ml volumetric flask. Then Milli-Q water is added to the mark.

8.3.4. Standard solutions

Standard solutions are prepared taking aliquots from the Phenol Red stock solution and solving them in sodium hydroxide 0.1 M in 100 ml volumetric flasks. This data is dispalyed in Table 8-1. However, a different set of solutions was made to characterize phenol red absorption spectrum. Originally a set of solutions were available from an older 4000 ppm stock solution and were utilized as tests to start designing the first procedures.

Standard Concentration (ppm)	Aliquot volume (ml)	NaOH volume (ml)
1	0.25	99.75
2	0.5	99.5
4	1	99
8	2	98
12	3	97
16	4	96
20	5	95

Table 8-1 Standard solutions

8.4. Detection systems characterization parameters

8.4.1. Limit of detection (LOD)

Detection limit is defined by the International Union of Pure and Applied Chemistry (IUPAC) in (Nič *et al.* 2009), as the smallest concentration of analyte that has a significantly larger signal than the signal from a suitable blank.

The LOD in most instrumental methods can be translated into the following expression:

$$S_{DL} = S_b + z\sigma_b$$ *Equation 8-1*

In Equation 8-1, S_{DL} is the analyte's detection limit, S_b is the average signal for blank, σ_b the blank's standard deviation and *z* is an integer.

8.4.2. Limit of quantization (LOQ)

(MacDougall and Crummett 1980) establish as a minimum criterion that the region for quantization should be clearly above the limit of detection. Equation 8-1 also describes the location of the LOQ.

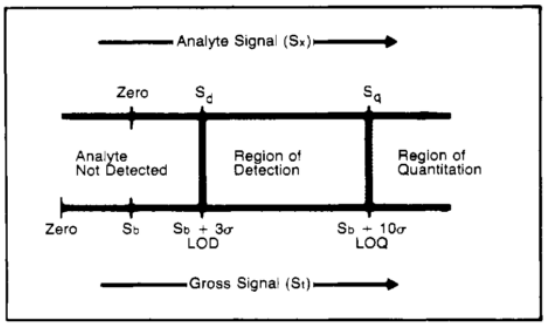

Figure 8-5 Regions of detection and quantization (MacDougall and Crummett 1980)

However, a distinction on *z* should be made in order to obey LOD's and LOQ's definitions. Figure 8-5 shows this difference: the border of the region of detection is at a distance $3\sigma_b$ from the blank average reported signal, and therefore, all values that fall below should be reported as non-detected. Values over $10\sigma_b$ are considered on the region of quantization.

8.5. Dispersion coefficient

Dispersion in flow systems was explained in section 4.3. In this segment, dispersion quantification will be addressed.

In both FIA and SIA techniques, zone sequencing and mutual dispersion of the zones are the key operations, as (Gubeli *et al.* 1991) state. For reagent-based chemistries, being optical methods amongst them, a mix between sample and reagent zones must be done in a suitable proportion and thus a medium dispersion has to be achieved. On the other hand, conductivity measurement requires limited dispersion.

The dispersion coefficient D is defined in (Gubeli *et al.* 1991) as the ratio of the concentration of the sample material before (C_0) and after (C) the dispersion process has taken place,

defining then Equation 8-2.

Equation 8-2

$$D = \frac{C_0}{C}$$

For a single compound, substituting Equation 5-4 into Equation 8-2 allows expressing dispersion in terms of absorbance (Equation 8-3), where A_0 is the absorbance before the dispersion process and A, after the phenomenon has taken place.

Equation 8-3

$$D = \frac{A_0}{A}$$

Electronic tongues are electrochemical sensor arrays; therefore dispersion coefficient must tend to 1, as (Gubeli *et al.* 1991) established. Plotting C/C_0 (D^{-1}) against injected volume leads to a theoretical curve similar to Figure 8-6.

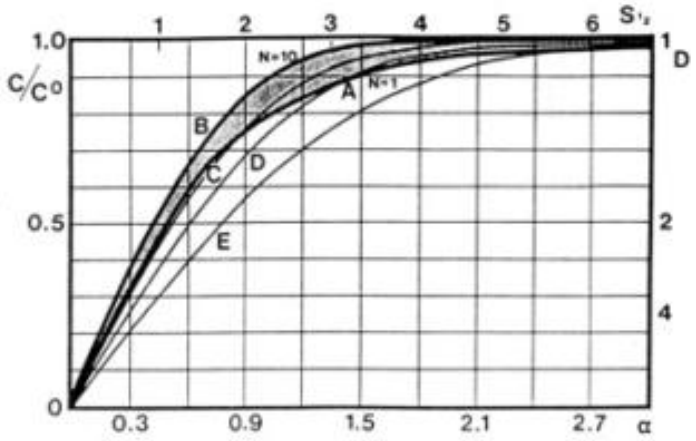

Figure 8-6 Theoretical curves for Dispersion coefficient vs volume(Gubeli *et al.* 1991)

9. Results and discussion

This section details all experiments and measurements made to achieve the objectives proposed in this project. Results can be grouped in three major categories. The first set of tests is developed outside the SIA system, using a basic FIA-like ensemble consisting of a peristaltic pump and the spectrometer in order to determine reagent characteristics and developing an operating procedure for the spectrometer.

The second category encloses all determinations required to calculate limits of detection and quantization. Moreover, the minimum volume needed to reach maximum absorbance will be found and automatic external calibration routines will be programmed.

The last series of trials will be targeted towards characterizing the mixing cell.

9.1. Phenol red characterization

This set of experiments was designed to obtain phenol red absorption spectrum to locate the maximum absorbance peak and set its location on the electromagnetic spectrum as the fixed wavelength for the absorbance measurements.

9.1.1. Preliminary tests

An old set of standards ranging 10^{-6} to 10^{-2} M phenol red concentration and a stock solution phenol red 0.011 M + NaOH 0.1M available from 2015-04-09 was used. For these tests, integration time was set to default (100 ms) and no averaging of data was made.

A full range spectrum, available in Figure 9-1 was measured. Although being highly noisy, some remarks were made.

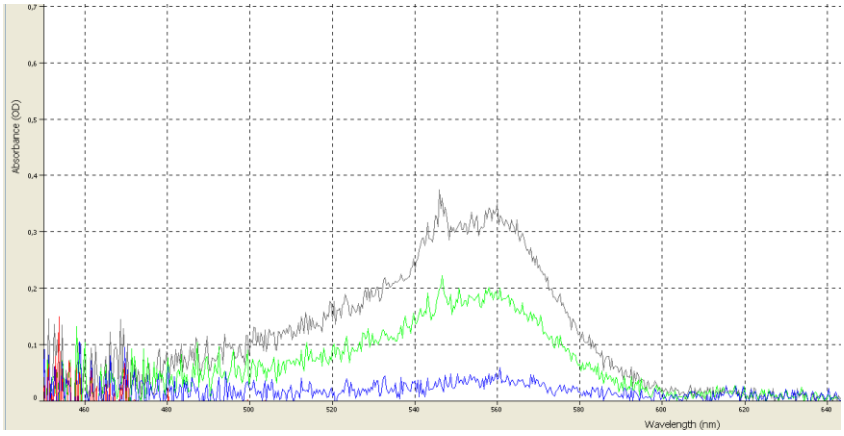

Figure 9-1 Phenol red preliminary absorption spectrum

During the tests, sample cell was not kept in the dark. Unlike traditional spectrometers, where samples are kept in a dark isolated compartment, Ocean View's calculating methods subtracting background spectrum from both sample and reference response (Equation 7-1) compensate the influence of external radiation. Thus another spectrum was recorded covering the flow cell.

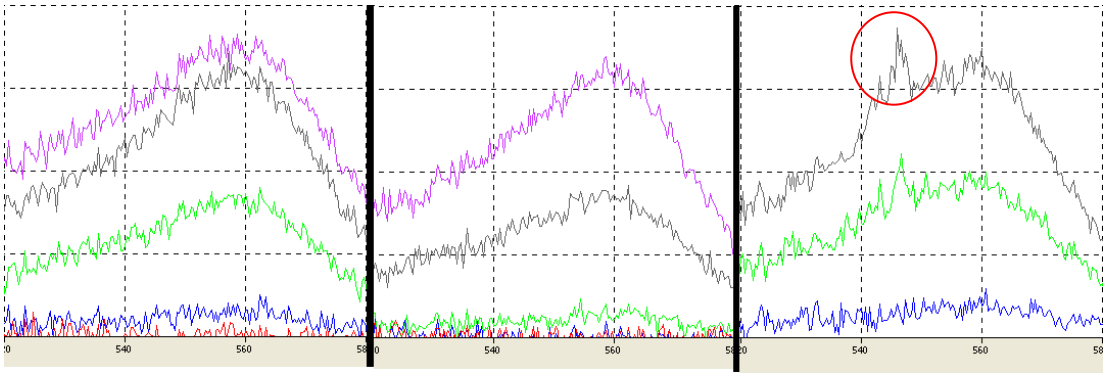

Figure 9-2 Left: covered cell. Center: Uncovered cell, lights off. Right: Uncovered cell

The indicated peak in Figure 9-2 disappeared after covering the cell with the canvas. It was suspected that fluorescent lightning radiation interfered in the measurements, so an additional test was made uncovering the cell and turning off the lights. Figure 9-2 shows the three spectrums, where distortion only appeared for the initial conditions.

Figure 9-3 displays the reference spectrums for both cell states: covered and uncovered. Background spectrum has been overlaid to reference spectrums to show at which wavelengths fluorescent lighting radiation affects.

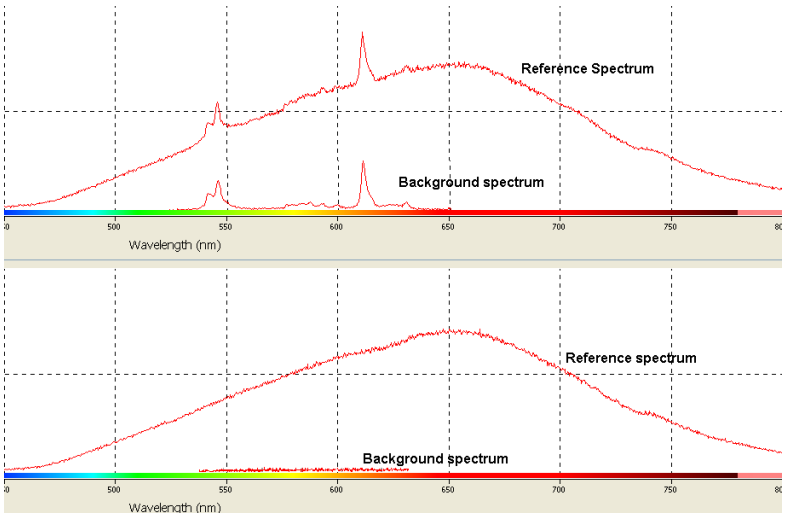

Figure 9-3 Reference and background spectrums: Top: Uncovered cell. Bottom: covered cell

While for the top situation background peaks are added to the reference line on the same

wavelength, keeping the cell in the dark generates a constant baseline with the same noise interval than the measurements. In order to smooth the data, five acquisitions were averaged.

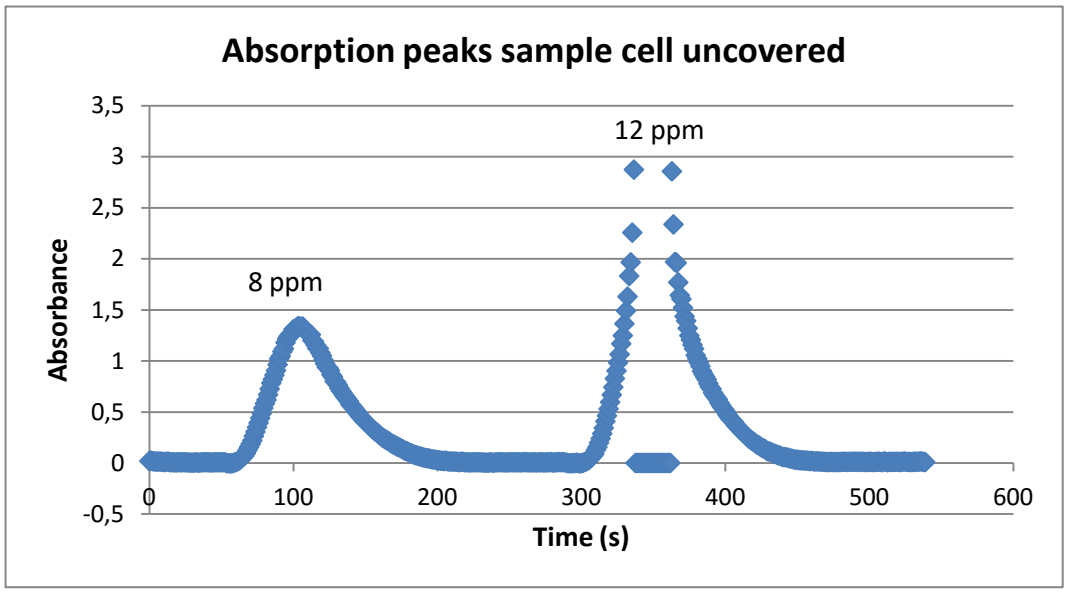

Figure 9-4 Absorption peaks when the simple cell is uncovered

Analyzing the spectrum obtained from an external calibration with the cell uncovered, shown in Figure 9-4, it was observed that absorbance values rose outside the linearity range (see section 9.2) and dropped suddenly to zero absorbance. This phenomenon can be attributed to fluorescent lighting radiation interfering in Equation 7-1. Finally it was decided to carry out all experiments keeping the cell isolated from fluorescent lightning.

9.1.2. Spectrometer comparison

In order to determine the maximum absorbance wavelength, new standards of concentration 2 to 40 ppm phenol red are prepared from the available stock solution. A full spectrum for 2, 10 and 40 ppm is measured with Flame spectrometer to determine the work wavelength. The results are displayed in Figure 9-5.

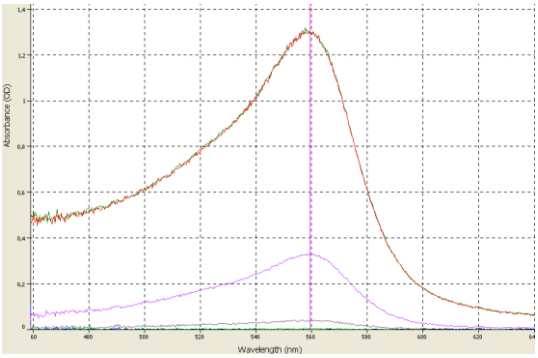

Figure 9-5 Phenol red spectrum for 2, 10, 40 ppm

The determined maximum peak with Flame spectrometer was located at 560 nm. As the procedure came from (del Mar 2004) (see section 8.1), a calibration curve with all standards, included in Figure 9-6 left was made at both 550 nm and 560 nm. Absorbance response adjusted better at 560 nm. The relative error between literature and experimental data is 1.81%. According to these results, the discrepancy between what (del Mar 2004) established and the analyzed experimental data in this project is within a 5% margin of error, which is totally acceptable.

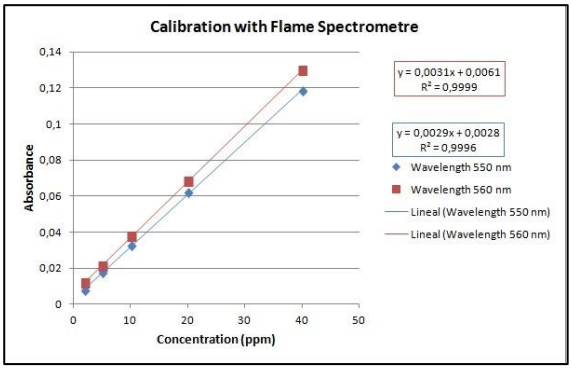

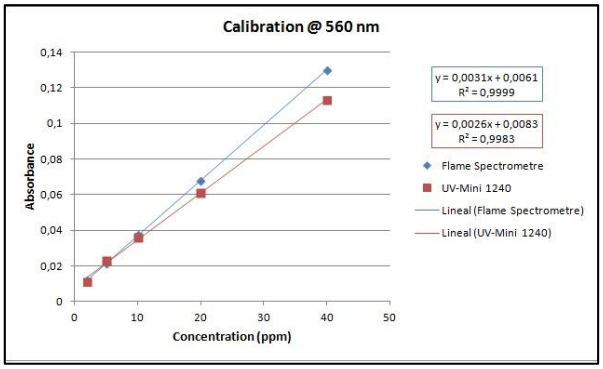

Figure 9-6 Left: Calibration curve for Flame spectrometer at 550 and 560 nm. Right: Calibration at fixed wavelength (560 nm) with Flame and UV-Mini 1240 spectrometers

Additionally, as a validation method for Flame spectrometer, a calibration curve was traced once again in a conventional spectrometer, the UV-Mini 1240 (Shimazdu), selecting wavelength at 560 nm. This calibration data is available in Figure 9-6. As observed, Flame spectrometer gave better response than UV-Mini 1240.

9.1.3. Sample degradation

(Vindevoghel 2005) in his project stated that phenol red standards were made once a week and kept in the dark. A set of standards from 2 to 20 ppm is made from the available stock. Its absorbance will be monitored through several days and its tendency will be observed. Results are plotted in Figure 9-7.

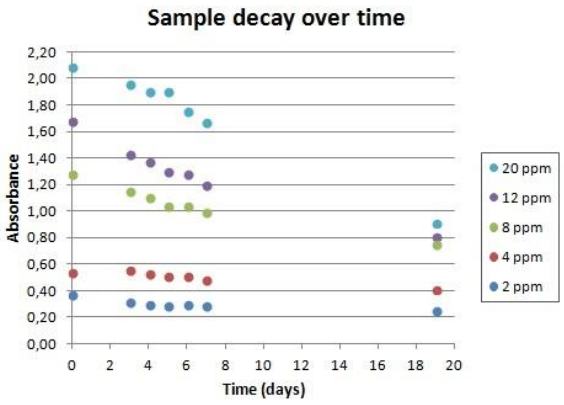

Figure 9-7 Sample decay over time

It is observed that absorbance measurements decrease as time passes further from the moment standards were prepared. It is also observed that decay rate for each standard is different. More concentrated solutions decay at a faster rate than less concentrated solutions. Consequently, stock solution must have suffered degradation since 2015-04-09 and thus, a new stock solution and set of standards will be made each week following methodology in section 8.3.

9.1.4. Selecting the set of standards

Originally, the series of standards contained the concentrations 2, 4, 8, 12, 20, 30, 40. For each, the absorbance spectrum was measured and is presented in Figure 9-8

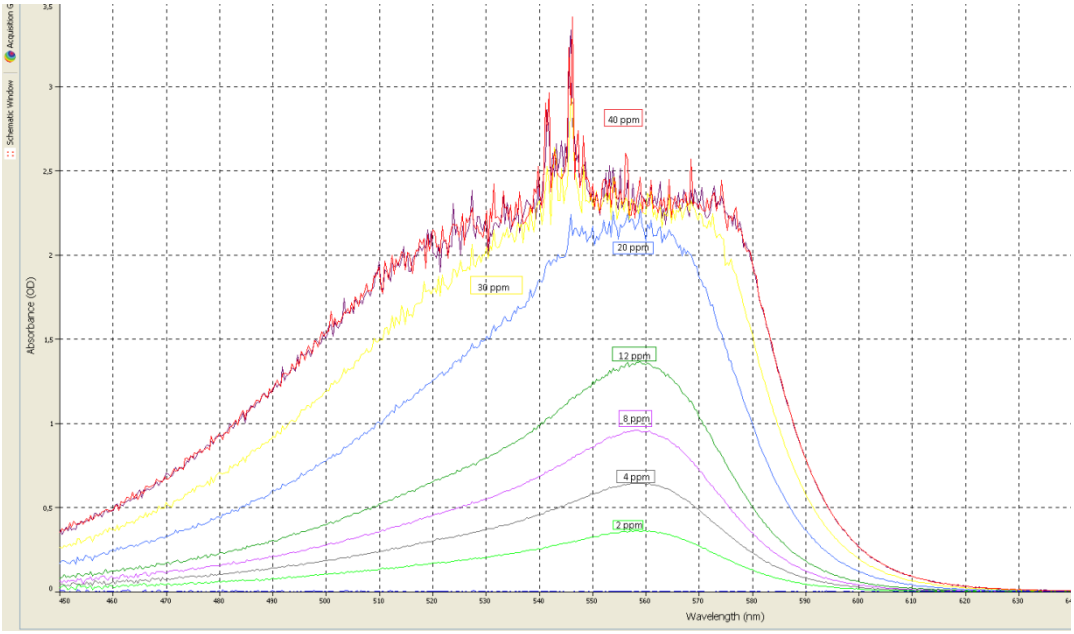

Figure 9-8 Standards' absorbance spectrum

It is visible that absorbance spectrum for standards 30 and 40 ppm is very noisy. Beer's law works best for diluted solutions where a linear correlation between absorbance and concentration can be established. Commonly, absorbance values superior to 1.5-2 are considered outside the linear range, so both standards were discarded. The calibration curve presented in Figure 9-9 shows how linearity starts to drop.

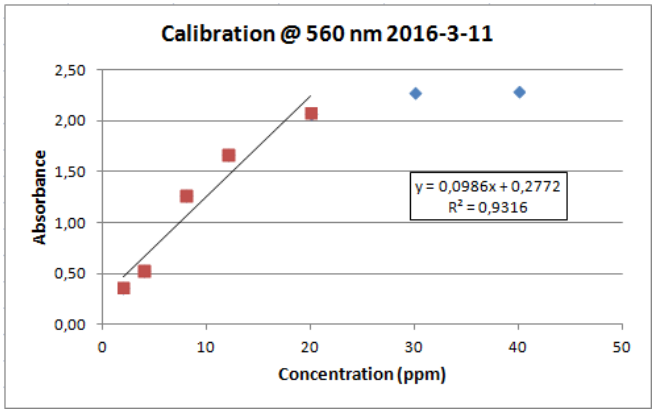

Figure 9-9 Original standards' calibration curve

However it was decided to keep the 20 ppm standard and introduce two new points corresponding to 1 ppm and 16 ppm in order to extend the study range.

9.2. External calibration

All experiments detailed in this segment are performed utilizing the SIA prototype. Scripts utilised for each determination will be named and the methodology will be explained. However script files will be presented in Annex 1. Spectrometer acquisition parameters will also be detailed for each determination.

9.2.1. Suitable flow rates

Usually, FIA and SIA systems work with flow rates from 1 ml/min to 5 ml/min. (Núñez 2016) studied the available and recommended range of velocities that could be set on the autoburette, and measured and tabulated the most suitable working flow rates for both 10 ml and 5 ml syringes. One of the recommended flow rates he established included in this interval was 1.2 ml/min. This value has been selected as the flow rate for aspiration as well as dispensation in all determinations.

9.2.2. SIA and Multivalve priming

Before running any experiments on the SIA prototype, general priming for all valves and tubes must be carried on. *SystemPriming.txt* will load the syringe with distilled water and

dispensations automatically opening all valves ensuring flow traverse all components. Additionally, a volume is loaded into the mixing cell and discharged afterwards.

When programming burette orders to load solutions through the multivalve ports it is presupposed that its tubing is completely filled of solution. *MultivalvePriming.txt* discharges the syringe into the distilled water tank (as the holding coil prevents any compound from reaching the burette). Next, a quarter of the syringe's total volume is aspirated from each port for entries 1-4. Last, distilled water dispensations through the mainline discharge the holding coil until absorbance drops to the baseline.

The process spectrum is represented in Figure 9-10.

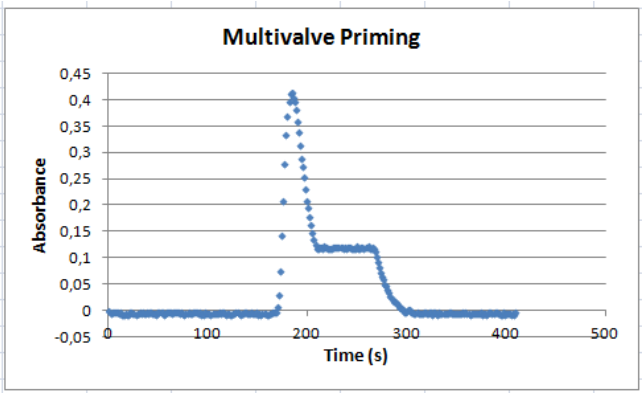

Figure 9-10 Multivalve priming

9.2.3. Determination of minimum volume

This experiment was designed to determine the minimum volume that must be injected into the system to obtain the maximum signal in absorbance at the same time ensuring that dispersion coefficient tends to the unit, as defined in section 8.5.

A set of injections of the 16 ppm phenol red solution will be analyzed. Injected volume starts at 25 µl and is pumped directly to the detection system. Several samples are injected increasing by 25 µl the aspirated volume until a final volume of 1100 µl. The absorbance of each injection will be measured to determine the minimum volume needed to achieve maximum absorbance.

To ensure peaks do not overlap and all colorant is carried out of the sampling cell additional 3.75 ml of distilled water are dispensed between each injection. This has been programmed in *MinVolumeTest.txt*.

For the spectrometer parameters, integration time was set automatically to 236.91 ms and the amount of scans to average was 6. Representing absorbance, obtained as the peak

height for each injection, versus the injected volume the curve in Figure 9-11.

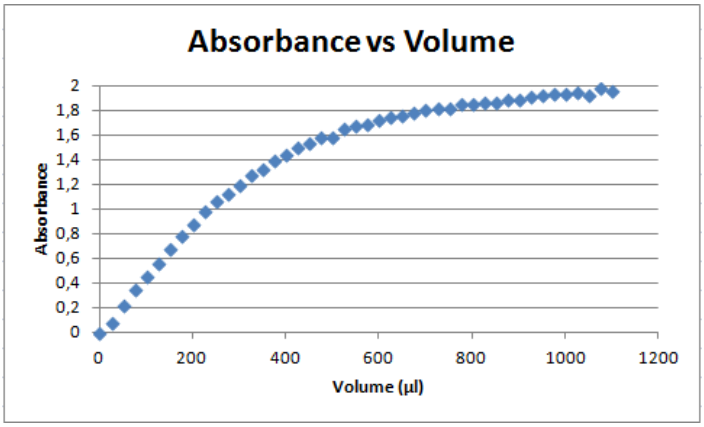

Figure 9-11 Absorbance for different injected volume

Applying Equation 8-3 to the points obtained, and defining A_0 as the maximum absorbance measured in Figure 9-11, the dispersion coefficient and the ratio of absorbance evolution can be studied for increasing volumes. Both parameters are plotted in Figure 9-12

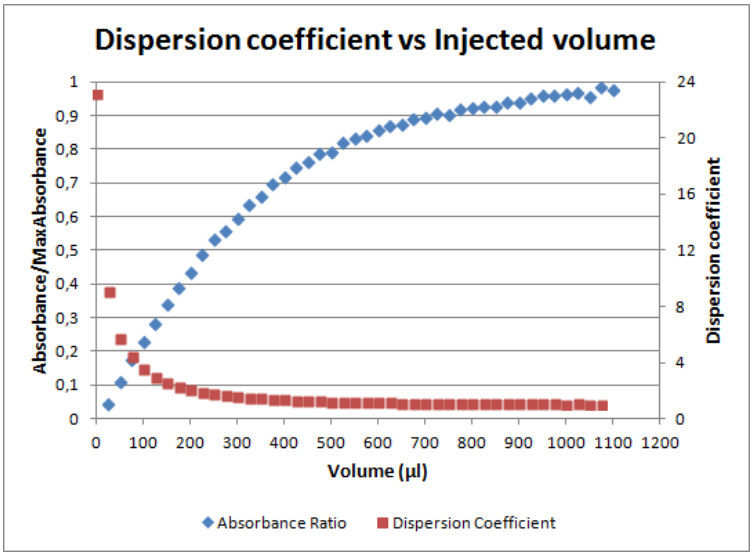

Figure 9-12 Absorbance ratio and dispersion coefficient

In order to determine the minimum volume that shall be injected in the SIA prototype to obtain acceptable response both, dispersion coefficient and absorbance ratio, must tend to 1. It is observed in Figure 9-12 that dispersion coefficient reaches its limit significantly faster than absorption ratio. For volumes larger than 925 µl both curves are inside a 5% discrepancy regarding the theoretical limit. In further determinations, sample volumes will be set to 1 ml.

9.2.4. Calibration curves

Calibration curves are drawn plotting the peak height for the absorbance of each of the standard solutions. Standards are sequentially injected and the next is not introduced in the system before its precedent has not been carried out.

All the calibration curves presented in this section are external calibrations. Standards are introduced into the SIA and then are sent directly to the detector system. Port 4 of the multivalve has always been reserved for carrier solution. All calibration sequences were made from the same script which has been evolving through the analysis of the spectral curves.

A volume of 0.5 ml of carrier is injected prior to the colorant aspiration in order to minimize dispersion inside the holding coil. Additionally, 50 µl of carrier are also aspirated after the colorant injection. Distilled water is injected afterwards to push the solutions through the SIA mainline. Calibration sequence is found in *CalibrationProcedure.txt*. An additional script, *CalibrationProcedureDualPeak.txt* was utilised for a few determinations that will be detailed later on in 9.2.7.

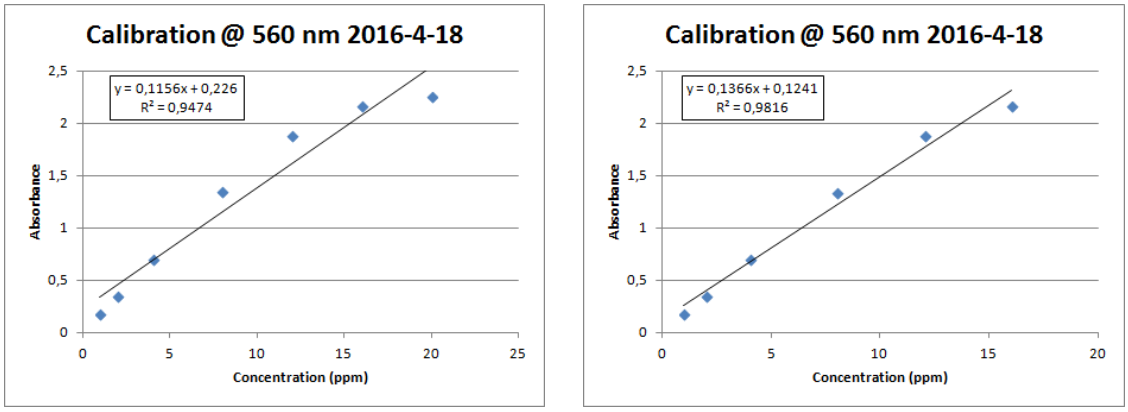

Figure 9-13 Calibration curves Left: 1-20 ppm Right: 1-16 ppm

One of the fundamental concepts in calibration is establishing the linearity range so the resultant curve can be described by Beer's Law. Two calibration curves are presented in Figure 9-13. It can be observed that regression coefficients improve excluding the 20 ppm standard in calibration as it starts to drift outside linearity. Thus the linearity range will be defined between 1 ppm and 16 ppm.

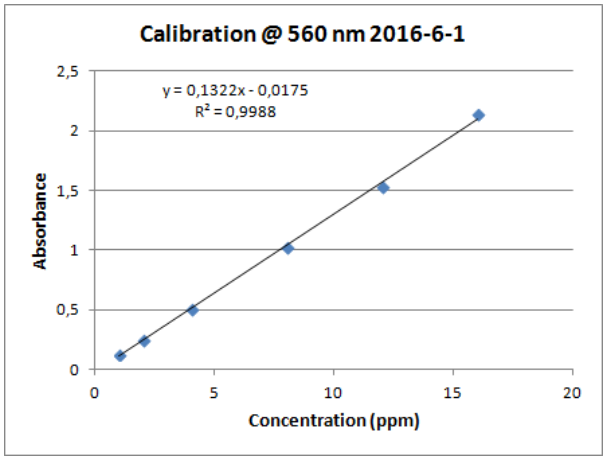

Figure 9-14 Calibration 2016-6-1

Although Beer's law curves intercept (0,0), regression fits displayed in Figure 9-13 and Figure 9-14 present a y-axis intercept deviation. This deviation on the regression models is due to the electronic noise produced during the usual operation of the spectrometer. Baseline oscillation will be detailed in 9.2.5.

Gathering all the calibration results during the project, a general absorptivity coefficient can be calculated. For a 95% confidence interval:

$$a = 0.1159 \pm 0.0055\ [cm^{-1} \cdot ppm^{-1}]$$

Nevertheless, as studied in 9.1.3, standards decay over time, thus absorptivity coefficient can be studied grouping calibrations by the amount of days passed since their preparation. Numerical data can be found in Table 9-1 and the intervals plotted in Figure 9-15.

Day	Mean	Confidence Interval
1	0.1313	(0.1145, 0.1481)
2	0.1160	(0.1014, 0.1306)
3	0.1226	(0.1161, 0.1292)
4	0.1069	(0.0955, 0.1182)
5	0.1051	(0.0881, 0.1220)

Table 9-1 Absorptivity confidence intervals

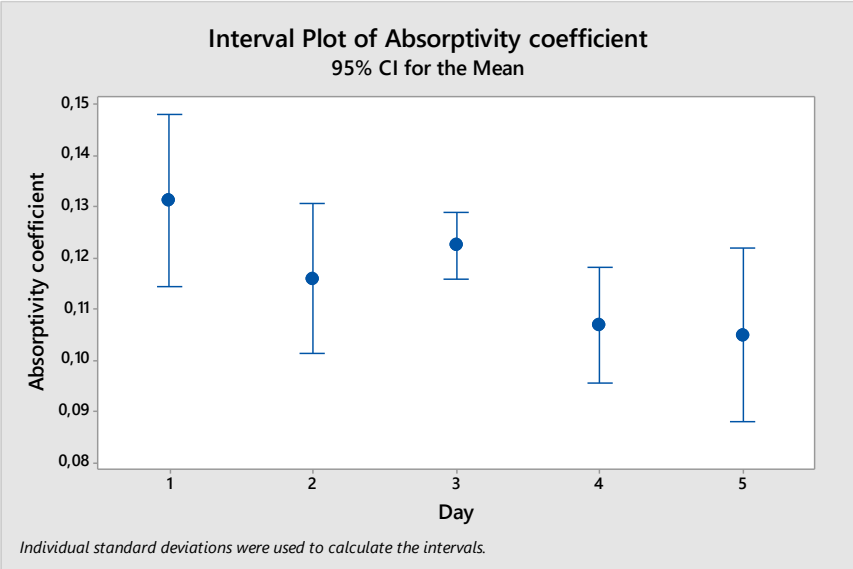

Figure 9-15 Confidence intervals for absorptivity over time

It can be observed in Figure 9-15 that the most significant drop in absorbance is produced between the first and second days. Utilizing ANOVA methods to compare the means of each group, with a value of α = 0.05, it is obtained that population means differ with a p-value of 0.015. When comparing the other groups excluding day 1 group, for a p-value of 0.052 means can be considered statistically equal.

9.2.5. Limit of Detection and Limit of Quantification

A set of blank measurements were registered between 15:53 pm to 15:57 pm, storing 157 acquisitions. Integration time was set automatically to 158.64 ms and 8 scans were averaged. Due to the large number of data, it is assumable that the sample's variance (*s)* approaches to the standard deviation of the blanks (σ). Blank's mean and σ, LOD and LOQ are calculated in Table 9-2.

Mean	0.0107
Standard Deviation	0.0015
LOD	0.0151
LOQ	0.0255

Table 9-2 Blank characterization

9.2.6. Peak Curves

When representing all data points acquired during a calibration in front of time, peak curves are drawn. Analyzing peak forms in these curves allows controlling if reagents are being adsorbed on the tubing walls, and the position of the samples inside the system can be inferred by peak form.

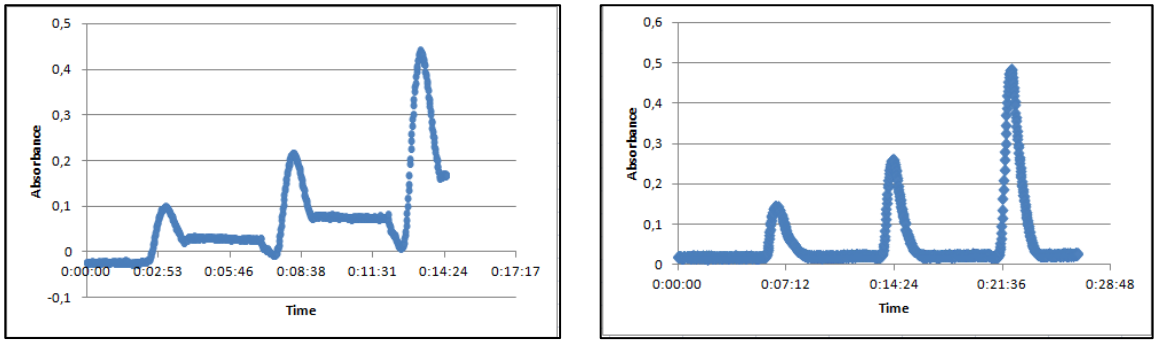

Figure 9-16 Peak curves comparison

In the Figure 9-16, a comparison of the peak curves for a calibration utilizing standards 1-4 ppm is shown. It was observed in the left curve that baseline was rising over time, and when the next peak arrived, a valley was generated and then absorbance started to increase. This phenomenon was due to the samples not being completely expulsed from the sample cell. One of the tails remained in the optical path. In the curve on the left, 500 µl distilled water were dispensed after the solution (curve on the right), In order to correct this problem 2050 µl water were dispensed.

9.2.7. Hydraulic hysteresis

In this section flow effects will be studied. It was observed that when autoburette finished the piston movements, flow was still affected by pressure and moved back when any valve was permuting. One solution to this phenomenon was to put waiting times after dispensations and aspirations. Coding 2 seconds reduced considerably the phenomena.

On the other hand, another study was realized referred to calibration mechanics. Calibrations peaks were duplicated and the standards order was reversed (downwards) to see if there was any influence or if the less concentrated solutions presented traces of the higher standards.

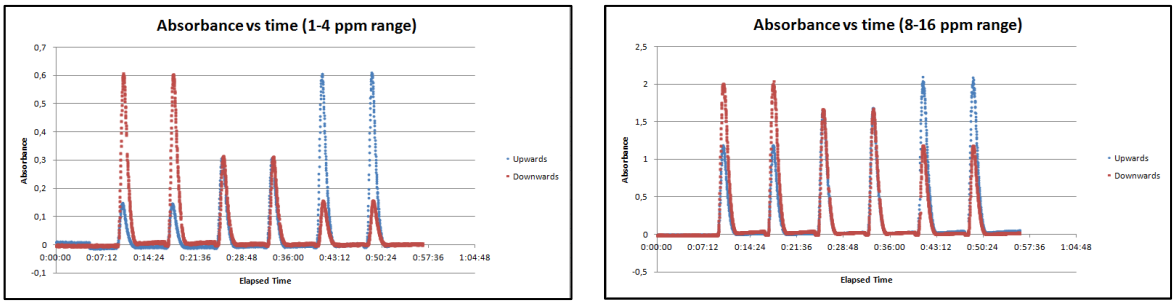

Figure 9-17 Upwards and downwards calibrations

Figure 9-17 shows the calibration curves for an upwards calibration (starting at 1 ppm) and a downwards calibration (starting at 16 ppm). No differences were observed between peak heights either between same concentration, same calibration and same concentration reverse calibration. It is concluded then, that both calibration directions are independently reliable.

9.2.8. Cleaning the system

Derived from analyzing peak forms like in 9.2.6, it was found that dispensing distilled water through mainline all reagents can be carried out of the system. The same script for priming the system can be utilised as a cleaning routine. However, passing a 0.1 M HNO_3 solution and then rinsing is recommended once a week.

Acid cleaning is recommended after long experiments to prevent reagent precipitation, especially if the flow is static for several hours. Otherwise, tubing or valves can be obstructed generating pressure necks when propelling flow, or vacuum bubbles in the syringe when aspiring, which can cause valve malfunctioning and the syringe glass to break.

9.3. Internal calibration

Internal calibration methods utilize the mixing cell to dilute a concentrated standard to the external calibration standards in order to being able to compare magnitudes.

9.3.1. Mixing cell preliminary tests

A set of experiments was designed to check the working conditions for the mixing cell. The 20 ppm standard was diluted to 50% dissolving it in NaOH carrier solution for a total volume of 4 ml. During the first group of trials, it was observed that when dispensing the same amount of aspirated fluid, tail traces remained in the holding coil. Agitation was set to 5 seconds. The method can be found in *Dilution50%M1M4.txt, Dilution50%M2M4.txt, Dilution50%M3M4.txt.*

(Escudé 2015) designed the tubing of the system. Between the multivalve and the mixing cell there are 435 mm of Teflon tubing 0.8 internal diameter, a volume of 874.6 µl volume. (Núñez 2016) stated that valves could be considered stagnant so the volume displacement inside can be negligible compared to the tubing volume. However, that is only true when valves have been primed. Cleaning the mixing cell requires removing all the fluid retained inside path from valve 7 to the mixing cell. An additional volume of 1000 µl was decided to be dispensed to compensate these volumes. However, half of that volume is dispensed after the phenol red solution and the rest after the carrier solution, allowing carrier solution to push colorant inside the cell.

Ports 1-3 of the multivalve were fed with the 20 ppm standard and entry 4 was reserved for NaOH carrier solution. Ten replicas for each port were made starting port 1 to port 3 and another ten replicas reversing the order. Dilution results are represented in Figure 9-18 and numerical data in Table 9-3.

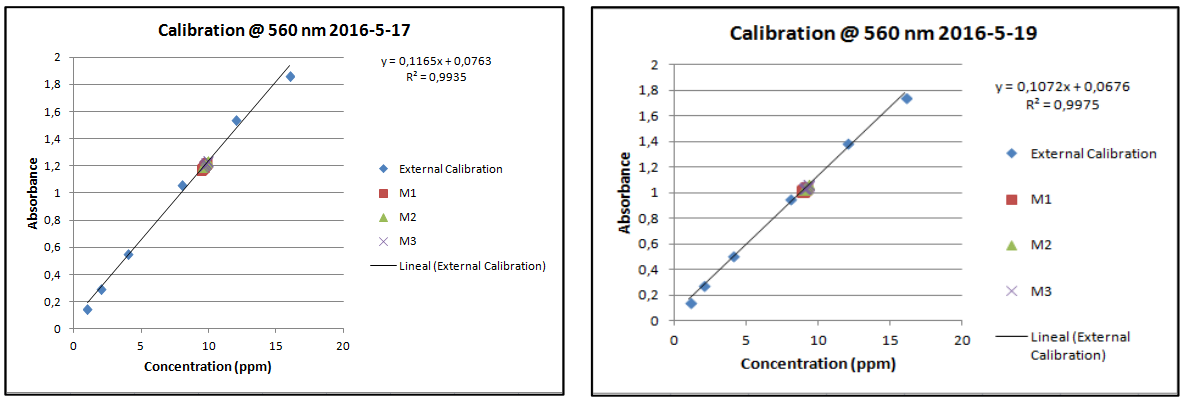

Figure 9-18 External calibration and 50 % dilutions Multivalve ports are labelled M1, M2, and M3 Left: Ascending order Right: Descending order

	Ascending		***Descending***	
	Concentration mean (ppm)	***StDev***	***Concentration mean (ppm)***	***StDev***
M1	*9.62*	*0.14*	*8.91*	*0.10*
M2	*9.72*	*0.02*	*9.00*	*0.11*
M3	*9.77*	*0.13*	*9.09*	*0.12*

Table 9-3 Concentrations obtained for 50% dilutions

Between both series of calibrations, no differences are found between M1, M2 and M3 series, as their means in each calibration are statistically equal. Thus there is no preference in injecting samples through a determined port. The drop in concentration is due to the decay of the standards two days after the ascending calibration.

9.3.2. Calibrating from 20 ppm standard

Under the same working conditions, and modifying the scripts utilised in section 9.3.1, a set of scripts is programmed to dilute the 20 ppm standard to the standards utilised for external calibration. These scripts are *20to1.txt, 20to2.txt, 20to4.txt, 20to8.txt, 20to12.txt* and *20to16.txt.*

Two replicas for two internal calibrations were made as for the first calibration carrier solution addition before colorant aspiration was not added. The calibrations are then represented with an external calibration in order to observe the deviations. Curves are presented in Figure 9-19.

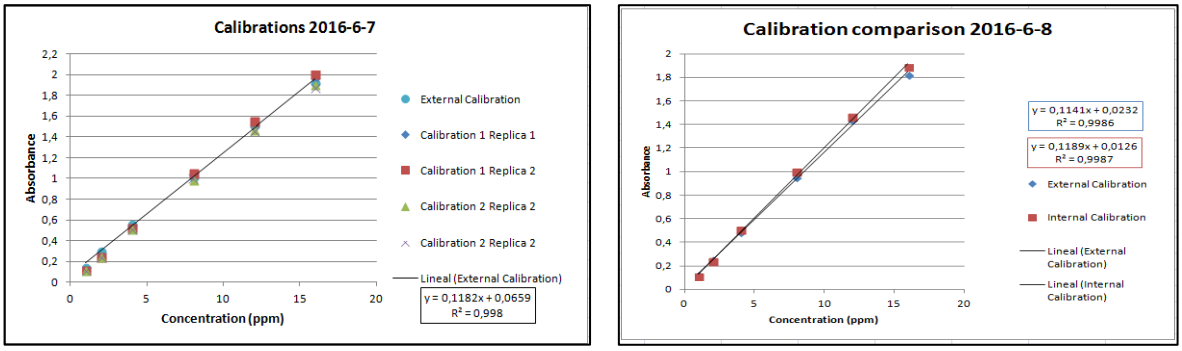

Figure 9-19 Internal calibrations using 20 ppm as stock solution

For the second calibration, the replicas were averaged and compared with a new calibration made the next day, as the experiment lasted all night. Therefore, calibration 1 approximates more accurately to 2016-6-7 calibration. It can be observed also in Figure 9-19 that small deviations appear for the least and most concentrated dilutions. For small volumes, colorant solution is more affected by dispersion as absorbance values fall below the external calibration while for concentrated samples, absorbance values are above the curve.

9.3.3. Calibrating from stock solution

Similarly to segment 9.3.2, the same procedure is applied utilizing the 400 ppm stock directly instead to make the dilutions. Scripts utilised follow the same instructions changing the volumes to maintain the dilution factor. These scripts are *400to1.txt, 400to2.txt, 400to4.txt, 400to8.txt, 400to12.txt* and *400to16.txt.*

Calibration curve is presented in Figure 9-20

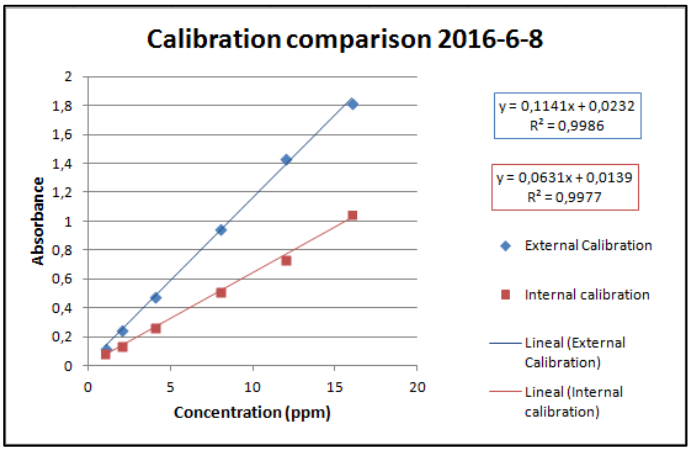

Figure 9-20 Calibration from stock solution

As observed in Figure 9-20, although internal calibration curve keeps linearity, high discrepancies are presented regards the external calibration. When recalculating the concentration of the diluted samples on the external calibration it was found that the dilution factor was twice the expected. This phenomenon could be described by two reasons. On the one hand, volumes required of the stock solution were inferior to 200 µl, which is the region of higher dispersion in Figure 9-12. On the other hand, a spectral displacement could have been produced since 10^{-5} M NaOH solvent was utilized against 0.1 M NaOH in the stock solution, altering the pH and thus, maximum absorbance wavelength.

9.3.4. Calibrating through successive dilutions

The objective for this trial was calibrating automatically the SIA prototype through the successive dilutions of the 400 ppm stock solution in the mixing cell. An aliquot from phenol red colorant solution was injected into the mixing cell. Carrier solution was added afterwards to dilute stock solution to 16 ppm and activating the stirrer. Following the agitation, a volume of sample is discharged from the cell and sent to the sample cell, leaving in the cell enough volume to reach the dilution to 12 ppm, repeating this process successively until a concentration of 1 ppm. Lastly the cell is cleand. Scripts for this process are *400to16.txt, 16to12.txt, 12to8.txt, 8to4.txt, 4to2.txt, 2to1.txt*.

The measured absorbance curves are plotted in Figure 9-21.

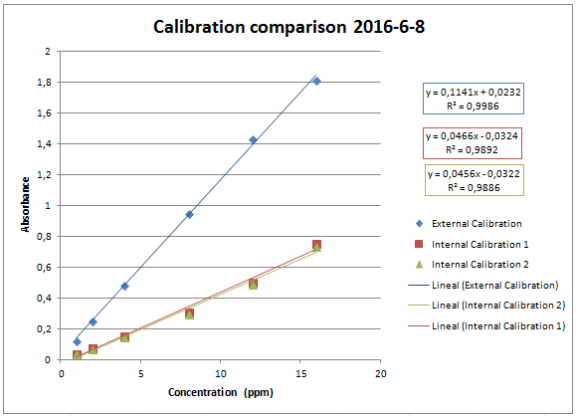

Figure 9-21 Successive dilution curves

As shown in Figure 9-21, and similar to Figure 9-20, successive dilutions calibration curves maintain linearity. However, discrepancies between internal and external calibration are far evident. This procedure is complex to monitor as compensation volumes must be added both to aspiration from the stirring cell as well as for dispensation into it. On the same manner for 9.3.3, the required volume from stock solution falls under the high dispersion coefficient region and pH also may be displacing the spectrum as dilutions are made utilizing carrier solution NaOH.

9.3.5. Cleaning the mixing cell

Maintaining the mixing cell clean from residual reagents is one of the key factors for the system's proper functioning. Analyzing absorbance for streams extracted from the stirring cell allows evaluating if any residual is found as the spectra would present peaks at determined wavelength, while if the stream is clean, which means the cell is clean, obtained spectroscopy data will measure only baseline absorption.

The designed script for cleaning the stirring cell, available in *CleaningMixingCell.txt*, was intended to reduce both water and time waste. When executing the script, the SIA empties the syringe to the distilled water tank. Next, a complete aspiration of the volume contained inside the mixing cell and the tubing between the cell and valve 6 is performed, ensuring that further additions will not bring back reagents.

Once the aspiration has ended, the mainline is rinsed through the detection system with two dispensations for a total volume of 7.5 ml. 2.5 ml are then dispensed into the mixing cell and the stirrer is activated for 10 seconds, dispersing reagents trapped under the magnet due to superficial tension. Mixing cell content is then discharged again through the mainline.

The absorption spectrum during a cleaning cycle is displayed in Figure 9-22. The first peak corresponds to the initial discharge from the mixing cell. The second corresponds to rinsing the cell.

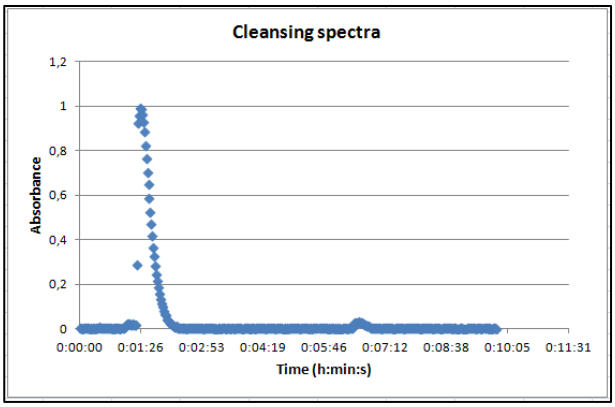

Figure 9-22 Cleaning spectral data

10. Budget

In this section project expenses are detailed in several categories.

- **Equipment**

  Equipment expenses are computed through amortization costs instead of the instrumental total cost. Amortization can be calculated as follows in Equation 10-1.

$$Amortization = \frac{Instrument\ Cost \cdot Use\ time}{Service\ Life}$$

Equation 10-1

  Other equipment (a computer and analytical balances) was utilized but is not included in this budget because it is considered fully amortized.

Concept	Cost [€]	Service Life [year]	Use time [years]	Amortization [€]
Flame S Spectrometer	2986.00	10	0.38	113.47
DH-Mini	1683.00	4.5	0.38	142.12
SMA-Z-10-UV	718.00	5	0.38	54.57
Optic Fibre 2x	390.00	10	0.38	14.82
SIA prototype	27180.46	10	0.20	543.61
Subtotal				**868.59**

- **Laboratory material**

Concept	Quantity	Unit cost [€]	Aggregated cost [€]
Volumetric flask 250 ml	1	37.10	37.10

Volumetric flask 100 ml	6	7.78	46.68
Volumetric flask 1000 ml	1	37.60	37.60
Beaker 150 ml	5	8.95	44.75
Subtotal			**166.13**

❖ **Reagents**

Concept	Distributor	SKU-Size	Cost [€]
Phenol red indicator, ACS reagent	Sigma-Aldrich	32661-10G	38.20
Sodium hydroxide puriss. p.a., ACS reagent, K ≤0.02%, ≥98.0% (T), pellets	Sigma-Aldrich	71690-1KG-D	28.50
Subtotal			**66.70**

❖ **Supplies**

Concept	Cost [€]
Water and electricity	500
Gloves (1 box 100 u.)	9.5
Paper	10
Subtotal	**519.5**

❖ **Total Costs**

Concept	Cost [€]
Equipment	868.59
Laboratory Material	166.13
Reagents	66.70
Supplies	519.5
Subtotal	1620.92
IVA (21%)	340.39
TOTAL	**1961.31**

11. Environmental considerations

In this project several environmental considerations have been taken account as the School's directives indicate for Degree Final Projects.

Sequential injection analysis systems reduce the environmental impact because the use of reagents is minimized as the process is automated and controlled electronically, therefore, more accurate.

Electronic tongues, though requiring training with a variety of standard sets, are less aggressive techniques than atomic absorption or other classical analytic methods.

However, during the experimentation of the project a large volume of residuals has been generated due to the degradation of the standards: a set of new solutions had to be prepared each week. After having developed the project for twenty weeks, an approximate volume of 62 liters of aqueous residue has been generated. Residual solutions were labeled under the category of Organic Colorant Reagents.

On the other hand, the final application of the prototype for monitoring biosorption processes will favour the optimization of this technique in long term, thus eliminating and recovering greater yields of heavy metals. Biosorption processes additionally reutilize agrarian residual to capture these metals.

Consequently, the benefits reported in optimizing biosorption processes as well as electronic tongues outcome the initial impact during the first phases of the design and implementation. Therefore, eliminating heavy metals through biosorption reduces the risk of biomagnification and rural residual are reutilised.

Conclusions

It was analyzed the influence of fluorescent lightning on the measurements by covering and uncovering the sample cell. Spectroscopic data determined that preserving the sample cell from fluorescent lighting is required.

Flame S Spectrometer reliability was contrasted comparing calibration curves with a conventional spectrometer (UV-Mini 1240).

It was determined that experimental maximum absorbance wavelength was 560 nm and it was within an acceptable 5% error margin from the literature values.

Phenol red standard solution degradation was measured through the evolution of its absorbance over a period of time. It was observed that concentrated solutions decayed faster.

A minimum volume of sample of 925 µl was determined to minimize dispersion effects into the carrier solution and the wash solution (distilled water), while limiting absorbance loss in less than the 5% of the maximum value.

1 ppm to 16 ppm linearity range was established analyzing the noise levels in spectral data and plotting calibration curves.

Reproducibility for external calibrations has been proved altering the order samples are injected.

The additional volume to compensate path length between multivalve and mixing cell was set in 1000 µl. Moreover, reproducibility has been tested, for different configurations. Therefore, It was found that injecting solutions was independent of the multivalve port the sample is located.

Internal calibration diluting a 20 ppm standard was set and its reliability has been confirmed when comparing data to the external calibration.

Scripts for standard operations including priming the system, calibrating and cleaning were programmed and verified obtaining peak curves usual in flow systems.

However, programming internal calibrations using the 400 ppm was not accomplished.

Future recommendations

Implementing LabVIEW and Ocean View under the same software interface would allow performing spectroscopic and electrochemical analysis with the sensor array simultaneously on the SIA system.

Valve 6 is connected in a sub optimal way: the normally open port has a lid for preventing fluid escaping. For long work sessions some fluid leakage is produced. Additionally, connecting the multivalve to the normally closed requires activating the valve for all operations which increases operation times.

Internal calibration diluting concentrated solutions should be studied further on. Perhaps testing on increasing concentrations from 20 ppm to 400 ppm can determine the maximum concentration internal calibration works up to.

Stirrer optimization could be studied more in detail if the knob that controls the motor had a reference system to know the rpm.

Additionally, a graduated scale for volume in the mixing cell would help verifying dispensations and aspirations in the cell.

Acknowledgements

First of all, I would like to express my gratitude towards Antonio Florido for providing me the opportunity of handling another project under his guidance, and towards his constant supervision as well as for providing necessary information regarding the project and all the patience shown especially on the first weeks preparing Phenol Red standards and allowing me to utilize additional equipment from academic laboratories.

I would also like to show gratitude to Sara, my parents and my brothers for supporting me during these years studying Degree in Chemical Engineering and encouraging me to continue advancing.

Last, but not least, thanks to Eric, Adrián, José Luis, Anabel, Eli and Cristina for sharing experiences in the laboratory.

Bibliography

Bibliographic references

AVE, D., 2015. Flame Miniature Spectrometer User Manual

BAXTER, P.J. and G.D. CHRISTIAN, 1996. Sequential Injection Analysis: A Versatile Technique for Bioprocess Monitoring. *Accounts of Chemical Research* [online], **29**(11), 515–521 Available from: http://pubs.acs.org/doi/abs/10.1021/ar950214z

CHRISTIAN, G.D., 2003. Flow analysis and its role and importance in the analytical sciences. *Analytica Chimica Acta*, **499**(1-2), 5–8

ESCUDÉ, B., 2015. (SIA), Optimització d'un sistema de monitorització de processos basat en anàlisi per injecció seqüencial

FIALAB, 2015. Fiber Optic SMA Z-Flow Cell Manual Design

GUBELI, T., G.D. CHRISTIAN and J. RUZICKA, 1991. Fundamentals of Sinusoidal Flow Sequential Injection Spectrophotometry. *Analytical Chemistry*, **63**, 2407–2413

HARVEY, D., 2009. Analytical Chemistry 2.0, 810

KIKAS, T., 2014. *Introduction to Flow Injection Analysis (FIA) Determination of Chloride Ion Concentration* [online] [viewed 6 Oct 2016]. Available from: ww2.chemistry.gatech.edu/class/analyt/fia.pdf

DE LAMO, D., 2014. Diseño y construcción del prototipo de un sistema de Análisis de Inyección Secuencial para la monitorización de procesos mediante lenguas electrónicas

LARSEN, D. and D. HARVEY, 2013. *Flow Injection Analysis* [online] [viewed 6 Dec 2016]. Available from: http://chemwiki.ucdavis.edu/Core/Analytical_Chemistry/Analytical_Chemistry_2.0/13_Kinetic_Methods/13.4:_Flow_Injection_Analysis

MACDOUGALL, D. and W.B. CRUMMETT, 1980. Guidelines for Data Acquisition and Data Quality Evaluation in Environmental Chemistry. *Analytical Chemistry* [online], **52**(14), 2242–2249 Available from: <Go to ISI>://WOS:A1980KT61200006

DEL MAR, B. i L.M., 2004. Nuevas Estrategias Para La Gestión de Fluidos En Sistemas Automatizados de Análisis. *Universitat Autònoma de Barcelona.* Universitat Autònoma de Barcelona

NIČ, M. *et al.*, eds., 2009. *IUPAC Compendium of Chemical Terminology* [online]. Research Triagle Park, NC: IUPAC [viewed 2 Jun 2016]. Available from: http://goldbook.iupac.org

NÚÑEZ, J.L., 2016. Estudio de la fluidica asociada a la optimización de un sistema de análisis por inyección secuencial (SIA)

NUÑEZ, L. *et al.*, 2013. Development and application of an electronic tongue for detection and monitoring of nitrate, nitrite and ammonium levels in waters. *Microchemical Journal* [online], **110**, 273–279 Available from: http://dx.doi.org/10.1016/j.microc.2013.04.018

PASEKOVA, H., M. POLASEK and P. SOLICH, 1999. Sequential injection analysis. *Chemické listy*, **93**(6), 354–359

PINTO, P.C.A.G. *et al.*, 2011. Sequential Injection Analysis Hyphenated with Other Flow Techniques: A Review. *Analytical Letters*, **44**(1-3), 374–397

ROBINSON, J.W., E.M. SKELLY FRAME and G.M. FRAME II, 2005. Undergraduate Instrumental analysis, **1**, 1079

SOCHACKA, J., 2015. Application of phenol red as a marker ligand for bilirubin binding site at subdomain IIA on human serum albumin. *Journal of photochemistry and photobiology. B, Biology* [online], **151**, 89–99 Available from: http://www.ncbi.nlm.nih.gov/pubmed/26231934

VINDEVOGHEL, W., 2005. Modification of a SIA-system by addition of a stirrer device (mixing flow cell)

Additional bibliographic references

AVE, D., 2015. Flame Miniature Spectrometer User Manual

BAXTER, P.J. and G.D. CHRISTIAN, 1996. Sequential Injection Analysis: A Versatile Technique for Bioprocess Monitoring. *Accounts of Chemical Research* [online], **29**(11), 515–521 Available from: http://pubs.acs.org/doi/abs/10.1021/ar950214z

CHRISTIAN, G.D., 2003. Flow analysis and its role and importance in the analytical sciences. *Analytica Chimica Acta*, **499**(1-2), 5–8

ESCUDÉ, B., 2015. (SIA), Optimització d'un sistema de monitorització de processos basat en anàlisi per injecció seqüencial

FIALAB, 2015. Fiber Optic SMA Z-Flow Cell Manual Design

GUBELI, T., G.D. CHRISTIAN and J. RUZICKA, 1991. Fundamentals of Sinusoidal Flow Sequential Injection Spectrophotometry. *Analytical Chemistry*, **63**, 2407–2413

HARVEY, D., 2009. Analytical Chemistry 2.0, 810

KIKAS, T., 2014. *Introduction to Flow Injection Analysis (FIA) Determination of Chloride Ion Concentration* [online] [viewed 6 Oct 2016]. Available from: ww2.chemistry.gatech.edu/class/analyt/fia.pdf

DE LAMO, D., 2014. Diseño y construcción del prototipo de un sistema de Análisis de Inyección Secuencial para la monitorización de procesos mediante lenguas electrónicas

LARSEN, D. and D. HARVEY, 2013. *Flow Injection Analysis* [online] [viewed 6 Dec 2016].

Available from: http://chemwiki.ucdavis.edu/Core/Analytical_Chemistry/Analytical_Chemistry_2.0/13_Kinetic_Methods/13.4:_Flow_Injection_Analysis

MACDOUGALL, D. and W.B. CRUMMETT, 1980. Guidelines for Data Acquisition and Data Quality Evaluation in Environmental Chemistry. *Analytical Chemistry* [online], **52**(14), 2242–2249 Available from: <Go to ISI>://WOS:A1980KT61200006

DEL MAR, B. i L.M., 2004. Nuevas Estrategias Para La Gestión de Fluidos En Sistemas Automatizados de Análisis. *Universitat Autònoma de Barcelona.* Universitat Autònoma de Barcelona

NIČ, M. *et al.*, eds., 2009. *IUPAC Compendium of Chemical Terminology* [online]. Research Triagle Park, NC: IUPAC [viewed 2 Jun 2016]. Available from: http://goldbook.iupac.org

NÚÑEZ, J.L., 2016. Estudio de la fluidica asociada a la optimización de un sistema de análisis por inyección secuencial (SIA)

NUÑEZ, L. *et al.*, 2013. Development and application of an electronic tongue for detection and monitoring of nitrate, nitrite and ammonium levels in waters. *Microchemical Journal* [online], **110**, 273–279 Available from: http://dx.doi.org/10.1016/j.microc.2013.04.018

PASEKOVA, H., M. POLASEK and P. SOLICH, 1999. Sequential injection analysis. *Chemické listy*, **93**(6), 354–359

PINTO, P.C.A.G. *et al.*, 2011. Sequential Injection Analysis Hyphenated with Other Flow Techniques: A Review. *Analytical Letters*, **44**(1-3), 374–397

ROBINSON, J.W., E.M. SKELLY FRAME and G.M. FRAME II, 2005. Undergraduate Instrumental analysis, **1**, 1079

SOCHACKA, J., 2015. Application of phenol red as a marker ligand for bilirubin binding site at subdomain IIA on human serum albumin. *Journal of photochemistry and photobiology. B, Biology* [online], **151**, 89–99 Available from: http://www.ncbi.nlm.nih.gov/pubmed/26231934

VINDEVOGHEL, W., 2005. Modification of a SIA-system by addition of a stirrer device (mixing flow cell)

Table of figures

Table of equations

Table index